TABLE 1. Antiprion effects of fucoidan mixed with infectious inoculum

Expt no.	Fucoidan concn in inoculum (μg/ml)	Incubation period (days) (mean ± SD) (n^c)	Statistical significance
Expt 1[a]	200	57.9 ± 2.5 (8)	$P < 0.05^d$
	20	55.0 ± 2.5 (6)	
	2	54.2 ± 2.7 (5)	
	0.2	54.2 ± 3.9 (6)	
	0.02	53.7 ± 2.6 (6)	
	0 (control)	53.0 ± 2.7 (6)	
Expt 2[b]	200	73.3 ± 3.7 (7)	$P < 0.01^e$
	20	67.4 ± 7.2 (5)	
	2	69.0 ± 2.1 (5)	
	0.2	66.8 ± 4.6 (6)	
	0.02	64.4 ± 4.5 (7)	
	0 (control)	62.2 ± 2.2 (6)	

[a] Twenty microliters of 1% 263K prion homogenate mixed with the designated dose of sample 2 fucoidan was inoculated intracerebrally into each Tg7 mouse immediately after the mixture was made.
[b] Twenty microliters of 0.1% 263K prion homogenate with the designated dose of sample 2 fucoidan was inoculated intracerebrally into each Tg7 mouse after the mixture was incubated for 14 h at room temperature.
[c] Number of mice tested in each group.
[d] Statistical significance against the value for the control, analyzed using one-way analysis of variance followed by the Tukey-Kramer method for multiple comparisons.
[e] Statistical significance against the value for either the 0.02 μg/ml group or the control, analyzed as described in footnote *d*.

TABLE 2. Prophylactic effects of fucoidan feeding preinfection or postinfection

Time of feeding	Fucoidan concn in feed (%)	Incubation period (days) (mean ± SD) (n^c)	Statistical significance
Preinfection[a]	2.5	215.4 ± 40.5 (5)	
	5	243.4 ± 31.8 (5)	
	10	212.2 ± 37.7 (5)	
Postinfection[b]	2.5	346.8 ± 28.0 (5)	$P < 0.01^d$
	5	368.1 ± 73.9 (7)	$P < 0.01^d$
	10	367.4 ± 44.9 (5)	$P < 0.01^d$
Control		231.1 ± 28.3 (6)	

[a] Fucoidan feeding started 7 days prior to enteral inoculation by gavage feeding with 200 μl of 10% 263K prion homogenate and ended the day before inoculation.
[b] Fucoidan feeding started the day after enteral inoculation and continued for 6 days.
[c] Number of mice tested in each group.
[d] Statistical significance against either the value for the preinfection group or the control, analyzed as described in Table 1, footnote *d*.

sarily responsible for the antiprion action of sulfated polysaccharides.

In one antiprion in vivo test, prion homogenate was mixed with a test compound prior to intracerebral inoculation and injected into the animal brain to elucidate increased incubation times attributable either to inactivation of the inoculum or its presence in the brain at the time of infection. Sample 2 was more effective in vitro. Therefore, it was tested in this manner using an animal model comprising hamster scrapie prion strain 263K and Tg7 mice expressing hamster PrP (16). That model was chosen because it gives the shortest incubation times of all experimental animal models available and because antiprion activity of fucoidan was observed, irrespective of prion strains. In an initial experiment, immediately after 20 μl of 1% 263K prion homogenate equivalent to an infectivity titer of about 10^8 50% lethal dose (LD_{50})/g of tissue (5) was mixed with sample 2 fucoidan at its final concentration of 0 to 200 μg/ml, five to eight-week-old Tg7 mice per group were inoculated intracerebrally with the mixture. Only the mixture containing the largest amount of sample 2 significantly increased the incubation period ($P < 0.05$) compared to that of the control (experiment 1 in Table 1).

Next, to determine whether preincubation of the mixture enhances inactivation of the infectious inoculum, the prion homogenate-fucoidan mixtures, similarly prepared but containing 10 times more diluted homogenate, were incubated for 14 h at room temperature and then injected similarly into five to seven mice per group. Experiment 2 in Table 1 shows that only the mixture containing the largest amount of sample 2 significantly increased the incubation period ($P < 0.01$), as demonstrated similarly in experiment 1. The findings suggest that fucoidan itself does not modify infectivity of the inoculum, but its presence in the brain might inhibit prion replication or PrP conversion, probably in a manner similar to that observed in vitro. This inference is supported by results described in previous reports that PPS is effective in delaying the onset of disease of prion-infected animals when administered continuously into the brain (5) or even by bolus shots (13). However, there remains another possibility, the possibility that fucoidan can modify the infectivity in the inoculum very rapidly without a 14-h incubation.

Finally, the potential practical utility of fucoidan was investigated, especially its prophylactic effects against peroral and enteral prion infections such as those that occur in BSE and vCJD. Two different timings of fucoidan feeding, where fucoidan powder was given in a mixture with feed powder at three different levels (2.5, 5, or 10%) were designed to reveal its distinct effects in mice. In one, fucoidan feeding started 7 days prior to enteral inoculation into five to seven Tg7 mice per group by gavage feeding over a few hours with a total of 200 μl of 10% 263K prion homogenate (about 10^9 LD_{50}/g infectivity titer) and ended the day preceding inoculation to elucidate its preinfection prophylactic effects. In the other, fucoidan feeding started the day after the inoculation and continued for 6 days to elucidate its postinfection prophylactic effects. The results demonstrated that fucoidan feeding that commenced after the enteral inoculation delayed the disease onset for about half the time of the control incubation (Table 2). However, fucoidan feeding before the enteral inoculation did not affect the incubation time.

Low proportions of fucoidan are absorbed from the gut into blood (11) and excreted in urine (10), although little more is known of the detailed pharmacology of ingested fucoidan. Sulfated polysaccharides injected intraperitoneally or intravenously inhibit prion replication in the lymphoreticular system, which is involved in the delivery of prion from the gut to the brain (8, 14). Therefore, it can be speculated that fucoidan absorbed into blood exerts its effects by inhibiting prion replication in the lymphoreticular system. A gap of fucoidan effects between the preinfection and postinfection fucoidan feeding might be attributable to the rapid clearance of blood fucoidan

into urine when this is the case. Another possible mechanism of the postinfectious fucoidan effects might be that it facilitates the excretion of infectious materials from the gut. This inference is supported by the fact that seaweed polysaccharides and other natural polysaccharides alter the bacterial spectrum of the gut and assist detoxification (9). In contrast, fucoidan does not seem to act via a certain factor induced in the host because fucoidan administered until the day before inoculation was never effective.

There was no difference in prolonged incubation times among the three different fucoidan concentrations, although the feed consumption per mouse was not statistically different in each experimental group irrespective of the fucoidan level. This might occur because even the lowest concentration of fucoidan in feed surpasses its absorption threshold from the gut or because blood fucoidan concentrations are not parallel to ingested fucoidan doses. The latter was previously reported in humans, where only a threefold difference in blood plasma fucoidan concentrations was detected despite a 7.5-fold difference in ingested fucoidan doses (11). In addition, the stoichiometric relationship between blood fucoidan concentration and inhibitory activity against prion replication in vivo might also be attributable to the results observed here. However, these inferences remain to be elucidated.

The inoculum used in the study of enteral infection contained an extremely high titer of about 10^9 LD_{50}/g, although most of the inoculum might be excreted in feces, and presumably, a much lower titer may cause the infection. More satisfactory prophylactic effects by orally ingested fucoidan might be expected when prion infection in BSE or vCJD is presumed to occur through a lower level of infectivity than that used in this study. On the other hand, the data presented cannot exclude the possibility that the in vivo effects of fucoidan on the 263K prion strain are different from those on other strains. However, this did not occur during our previous experiments with a sulfated polysaccharide (5).

Finally, all fucoidan samples used here contained fucoidan at less than 90% of total weight. Therefore, it is possible that ingredients other than fucoidan exert the antiprion activity observed in this study. However, gel-filtrated samples, which contained 99.9% fucoidan with a mass of 100 to 190 kDa produced the same in vitro results (data not shown). Therefore, fucoidan itself of the dietary brown seaweed imparts the antiprion activity. Its daily ingestion has the potential to provide some prophylactic benefit against such oral or enteral prion infections as occurred in BSE and vCJD, but further studies must be done to elucidate the pharmacology of ingested fucoidan.

This work was supported by the Ministry of Health, Labor and Welfare (H16-kokoro-024) and the BSE Control Project of the Ministry of Agriculture, Forestry and Fisheries of Japan.

We thank Satoshi Kawatake for valuable suggestions and Kyomi Sasaki for manuscript preparation.

REFERENCES

1. **Adjou, K. T., S. Simoneau, N. Salès, F. Lamoury, D. Dormont, D. Papy-Garcia, D. Barritault, J. P. Deslys, and C. I. Lasmézas.** 2003. A novel generation of heparan sulfate mimetics for the treatment of prion diseases. J. Gen. Virol. **84**:2595–2603.
2. **Berteau, O., and B. Mulloy.** 2003. Sulfated fucans, fresh perspectives: structures, functions, and biological properties of sulfated fucans and an overview of enzymes active toward this class of polysaccharide. Glycobiology **13**:29R–40R.
3. **Cashman, N. R., and B. Caughey.** 2004. Prion diseases–close to effective therapy? Nat. Rev. Drug Discov. **3**:874–884.
4. **Caughey, B., K. Brown, G. J. Raymond, G. E. Katzenstein, and W. Thresher.** 1994. Binding of the protease-sensitive form of PrP (prion protein) to sulfated glycosaminoglycan and Congo red. J. Virol. **22**:163–167.
5. **Doh-ura, K., K. Ishikawa, I. Murakami-Kubo, K. Sasaki, S. Mohri, R. Race, and T. Iwaki.** 2004. Treatment of transmissible spongiform encephalopathy by intraventricular drug infusion in animal models. J. Virol. **78**:4999–5006.
6. **Doh-ura, K., K. Tamura, Y. Karube, M. Naito, T. Tsuruo, and Y. Kataoka.** 19 January 2007. Chelating compound, chrysoidine, is more effective in both antiprion activity and brain endothelial permeability than quinacrine. Cell. Mol. Neurobiol. doi:10.1007/s10571-006-9122-0.
7. **Doh-Ura, K., T. Iwaki, and B. Caughey.** 2000. Lysosomotropic agents and cysteine protease inhibitors inhibit scrapie-associated prion protein accumulation. J. Virol. **74**:4894–4897.
8. **Farquhar, C., A. Dickinson, and M. Bruce.** 1999. Prophylactic potential of pentosan polysulphate in transmissible spongiform encephalopathies. Lancet **353**:117.
9. **Fitton, J. H.** 2003. Brown marine algae: a survey of therapeutic potentials. Altern. Complem. Ther. **9**:29–33.
10. **Guimarães, M. A. M., and P. A. S. Mourão.** 1997. Urinary excretion of sulfated polysaccharides administered to Wistar rats suggests a renal permselectivity to these polymers based on molecular size. Biochim. Biophys. Acta **1335**:161–172.
11. **Irhimeh, M. R., J. H. Fitton, R. M. Lowenthal, and P. Kongtawelert.** 2005. A quantitative method to detect fucoidan in human plasma using a novel antibody. Methods Find. Exp. Clin. Pharmacol. **27**:705–710.
12. **Ishikawa, K., Y. Kudo, N. Nishida, T. Suemoto, T. Sawada, T. Iwaki, and K. Doh-ura.** 2006. Styrylbenzoazole derivatives for imaging of prion plaques and treatment of transmissible spongiform encephalopathies. J. Neurochem. **99**:198–205.
13. **Kocisko, D. A., W. S. Caughey, R. E. Race, G. Roper, B. Caughey, and J. D. Morrey.** 2006. A porphyrin increases survival time of mice after intracerebral prion infection. Antimicrob. Agents Chemother. **50**:759–761.
14. **Mabbott, N. A., and G. G. MacPherson.** 2006. Prions and their lethal journey to the brain. Nat. Rev. Microbiol. **4**:201–211.
15. **Nagaoka, M., H. Shibata, I. Kimura-Takagi, S. Hashimoto, K. Kimura, T. Makino, R. Aiyama, S. Ueyama, and T. Yokokura.** 1999. Structural study of fucoidan from *Cladosiphon okamuranus Tokida*. Glycoconjugate J. **16**:19–26.
16. **Race, R. E., S. A. Priola, R. A. Bessen, D. Ernst, J. Dockter, G. F. Rall, L. Mucke, B. Chesebro, and M. B. Oldstone.** 1995. Neuron-specific expression of a hamster prion protein minigene in transgenic mice induces susceptibility to hamster scrapie agent. Neuron **15**:1183–1191.
17. **Rainov, N. G., I. R. Whittle, and K. Doh-ura.** 2005. Treatment options in patients with prion disease—the role of long term cerebroventricular infusion of pentosan polysulphate, p. 41–66. *In* T. Kitamoto (ed.), Prions—food and drug safety. Springer-Verlag, Tokyo, Japan.
18. **Safar, J., H. Wille, V. Itri, D. Groth, H. Serban, M. Torchia, F. E. Cohen, and S. B. Prusiner.** 1998. Eight prion strains have PrP^{Sc} molecules with different conformations. Nat. Med. **4**:1157–1165.
19. **Schonberger, O., L. Horonchik, R. Gabizon, D. Papy-Garcia, D. Barritault, and A. Taraboulos.** 2003. Novel heparan mimetics potently inhibit the scrapie prion protein and its endocytosis. Biochem. Biophys. Res. Commun. **312**:473–479.
20. **Shyng, S. L., S. Lehmann, K.L. Moulder, and D. A. Harris.** 1995. Sulfated glycans stimulate endocytosis of the cellular isoform of the prion protein, PrP^{C}, in cultured cells. J. Biol. Chem. **270**:30221–30229.
21. **Taylor, D. M.** 2002. Current perspectives on bovine spongiform encephalopathy and variant Creutzfeldt-Jakob disease. Clin. Microbiol. Infect. **8**:332–339.

JOURNAL OF VIROLOGY, Dec. 2007, p. 12889–12898
0022-538X/07/$08.00+0 doi:10.1128/JVI.01563-07

Vol. 81, No. 23

Orally Administered Amyloidophilic Compound Is Effective in Prolonging the Incubation Periods of Animals Cerebrally Infected with Prion Diseases in a Prion Strain-Dependent Manner▽

Yuri Kawasaki,[1] Keiichi Kawagoe,[2] Chun-jen Chen,[2] Kenta Teruya,[1] Yuji Sakasegawa,[1] and Katsumi Doh-ura[1]*

Department of Prion Research, Tohoku University Graduate School of Medicine, Sendai, Japan,[1] and Tokyo R & D Center, Daiichi Pharmaceutical Co., Ltd., Tokyo, Japan[2]

Received 18 July 2007/Accepted 4 September 2007

The establishment of effective therapeutic interventions for prion diseases is necessary. We report on a newly developed amyloidophilic compound that displays therapeutic efficacy when administered orally. This compound inhibited abnormal prion protein formation in prion-infected neuroblastoma cells in a prion strain-dependent manner: effectively for RML prion and marginally for 22L prion and Fukuoka-1 prion. When the highest dose (0.2% [wt/wt] in feed) was given orally to cerebrally RML prion-inoculated mice from inoculation until the terminal stage of disease, it extended the incubation periods by 2.3 times compared to the control. The compound exerted therapeutic efficacy in a prion strain-dependent manner such as that observed in the cell culture study: most effective for RML prion, less effective for 22L prion or Fukuoka-1 prion, and marginally effective for 263K prion. Its effectiveness depended on an earlier start of administration. The glycoform pattern of the abnormal prion protein in the treated mice was modified and showed predominance of the diglycosylated form, which resembled that of 263K prion, suggesting that diglycosylated forms of abnormal prion protein might be least sensitive or resistant to the compound. The mechanism of the prion strain-dependent effectiveness needs to be elucidated and managed. Nevertheless, the identification of an orally available amyloidophilic chemical encourages the pursuit of chemotherapy for prion diseases.

Transmissible spongiform encephalopathies, or prion diseases, are a group of fatal neurodegenerative disorders that include Creutzfeldt-Jakob disease (CJD) and Gerstmann-Sträussler-Scheinker syndrome (GSS) in humans and scrapie, bovine spongiform encephalopathy, and chronic wasting disease in animals. These disorders are characterized by accumulation in the brain of an abnormal isoform of prion protein (PrP), which is a main component of the pathogen, prion, or a pathogen itself and which is rich in beta-sheet structure and resistant to digestion with proteinase K (24). Recent outbreaks of variant CJD and iatrogenic CJD through use of cadaveric growth hormone or dura grafts in younger people have necessitated the development of suitable therapies.

Caughey and colleagues first found Congo red and sulfated glycans to inhibit abnormal PrP formation in vitro (5, 6), although Congo red was much earlier described as a staining device for prion amyloid rods (23). Since the discovery of the therapeutic activity of Congo red, amyloidophilic compounds such as amyloid dye derivatives and glucoseaminoglycan mimetics have been noted as one class of possible therapeutic candidates for prion diseases (4, 32). Recently, the most advanced progress with amyloidophilic compounds, which have an excellent ability to permeate through the blood-brain barrier, has been made in the field of diagnosis of Alzheimer's disease. Some amyloidophilic compounds are developed as imaging probes to visualize amyloid deposits in the brains of Alzheimer's disease patients using positron emission tomography or single-photon emission computed tomography technology (3). Some of these chemicals are also useful to visualize abnormal PrP amyloids of some types of prion diseases in the brain (2, 14, 15, 28, 30).

We previously reported that some of these amyloid-imaging probes are effective as antiprion compounds and prolong the incubation periods of animals cerebrally infected with prion disease (14). We also reported that a new class of amyloidophilic chemicals, styrylbenzoazole derivatives, which have better penetration through the blood-brain barrier and which show more discrete labeling of amyloid deposition in brain tissues affected by either Alzheimer's disease or prion diseases, are effective as antiprion chemicals (15, 19). However, the efficacy of these amyloidophilic compounds, intravenously administered weekly, was not remarkable but was rather limited. In addition, their effectiveness was suggested to be prion strain dependent, but this was not fully evaluated because of the limited availability of the compounds in quantity and dosing route. It can be assumed that elevated brain chemical levels are necessary for a compound's efficacy. Therefore, a multiple-dosing regimen, which causes more sustained elevation in brain chemical levels, might be preferable to a single weekly dosing. In this study, to ascertain undefined benefits and limitations of amyloidophilic compounds as therapeutic drug candidates for prion diseases, a new class of amyloidophilic compounds which have no similarity in chemical structure with previously reported antiprion compounds was synthesized and tested for either antiprion activity in vitro or therapeutic efficacy in vivo when administered orally as a mixture with feed.

* Corresponding author. Mailing address: Department of Prion Research, Tohoku University Graduate School of Medicine, 2-1 Seiryo-cho, Aoba-ku, Sendai, Miyagi 980-8575, Japan. Phone: 81-22-717-8232. Fax: 81-22-717-7656. E-mail: doh-ura@mail.tains.tohoku.ac.jp.

▽ Published ahead of print on 19 September 2007.

TABLE 1. Tested compounds and their inhibition of abnormal PrP formation in ScN2a cells

Compound	Chemical structure	Mol wt	Octanol-water distribution coefficient[a] (log $D_{6.8}$)	Inhibition of abnormal PrP (approximate EC_{50}, nM)[b]	Maximum tolerance dose[c] (μM)
cpd-B	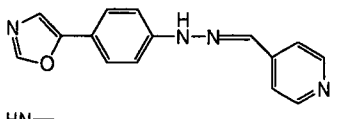	264	4.1	0.06	>10
cpd-D1	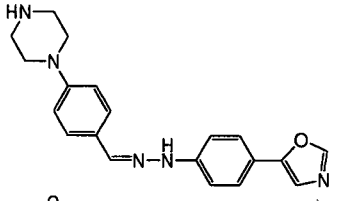	347	2.2	100	>10
cpd-D2	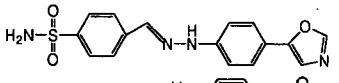	342	3.6	10	>10
cpd-D3	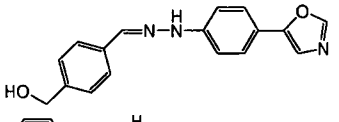	293	3.2	1	>10
cpd-D4	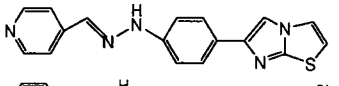	319	Not determined	1	>10
cpd-D5	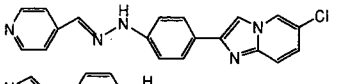	347	4.7	1	>10
cpd-D6	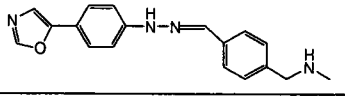	306	2.4	10	>10

[a] The distribution coefficient, a measure of a compound's hydrophilicity or hydrophobicity, was estimated using ChemAxon's calculator plugin software (Budapest, Hungary). The coefficients of medicines used for brain diseases are generally around 3.0.
[b] The approximate dose giving 50% inhibition of abnormal PrP formation relative to the control.
[c] The maximal dose that does not affect the rate of cell growth to confluence.

MATERIALS AND METHODS

Chemicals and experimental models. Test compounds were synthesized at the Tokyo R & D Center of Daiichi Pharmaceutical Co., Ltd. (Tokyo, Japan). The structures of the compounds are shown in Table 1. The compounds were dissolved in 100% dimethyl sulfoxide using ultrasonication and stored at −30°C until use.

Cultured cells were grown in Opti-MEM (Invitrogen Corp., Carlsbad, CA) supplemented with 10% fetal calf serum. As cellular models for the screening of antiprion compounds, either mouse neuroblastoma cells (N2a cells) or N2a cells with fivefold PrP overexpression (N2a-58 cells) which were persistently infected with a distinct prion strain were used, as follows: N2a cells infected with RML scrapie prion (ScN2a cells) (25), N2a cells with 22L scrapie prion (N167 cells), N2a-58 cells with RML scrapie prion (N002 or Ch2 cells), or N2a-58 cells with Fukuoka-1 GSS prion (F3 cells) (15). The Ch2 cells are a subclone of N002 cells.

Five-week-old Tga20 mice overexpressing murine PrP (11) or Tg7 mice overexpressing hamster PrP (26) were used as animal disease models after intracerebral infection with 20 μl of 1% (wt/vol) brain homogenate of RML prion, 22L prion, or Fukuoka-1 prion for Tga20 mice or 263K scrapie prion for Tg7 mice. Five-week-old ICR mice and Syrian hamsters were also used after they were infected intracerebrally with 20 μl of 1% (wt/vol) brain homogenate of RML prion or 40 μl of 1% (wt/vol) brain homogenate of 263K prion, respectively. Each animal was maintained under deep ether anesthesia for minimum distress during intracerebral inoculation. Permission for the animal study was obtained from the Animal Experiment Committee of Tohoku University, Japan.

In vitro PrP imaging. Autopsy-diagnosed brain samples from cases of GSS, which were kindly provided by Toru Iwaki from the Department of Neuropathology, Kyushu University, Japan, were used. After fixation in 10% buffered formalin for 2 weeks, the sample was immersed in 98% formic acid for reduction of prion infectivity, embedded in paraffin, and cut into 7-mm-thick sections. For neuropathological staining, deparaffinized sections were immersed in 1% Sudan black solution to quench tissue autofluorescence. They were then incubated for 30 min in 1 mM solution of compound B (cpd-B), rinsed with distilled water, and examined under a fluorescence microscope (DMRXA; Leica Microsystems GmbH, Wetzlar, Germany) using a fluorescein isothiocyanate filter set.

For comparison, each section was subsequently immunostained for PrP as described in a previous study (7). Briefly, the sections were treated with a hydrolytic autoclave and incubated with a rabbit primary antibody, anti-PrP-C, which was raised against a mouse PrP fragment consisting of amino acids 214 to 228 (1:200; Immuno-Biological Laboratories Co. Ltd., Gunma, Japan), followed by incubation with EnVision+System horseradish peroxidase labeling polymer (Dako, Glostrup, Denmark). The reaction product was developed with 3,3'-diaminobenzidine tetrahydrochloride solution and counterstained with hematoxylin.

In vitro treatment in cell cultures. Antiprion activity was evaluated by assaying the content of protease-resistant PrP (PrPres) in the cellular models, as described in earlier studies (6, 8, 18). Briefly, test compounds were added at the designated concentrations when cells were passaged at 10% confluence, while maintaining the final concentration of dimethyl sulfoxide in the medium at less than 0.5%. The cells were allowed to grow to confluence and were lysed with lysis buffer (0.5% sodium deoxycholate, 0.5% Nonidet P-40, phosphate-buffered saline [PBS]). For analysis of PrPres, samples were digested using 10 μg/ml proteinase K for 30 min at 37°C; the digestion was stopped using 1 mM phenylmethylsulfonyl fluoride. The samples were centrifuged at 100,000 × *g* for 30 min, and then pellets were resuspended in 1× sample loading buffer and boiled for 5 min. For analysis of the total level of cellular PrP in N2a cells treated with a test compound, cell lysates were mixed directly with one-quarter volume of 5× sample loading buffer and boiled for 5 min.

The samples were analyzed by immunoblotting. They were separated by electrophoresis on a 15% Tris-glycine–sodium dodecyl sulfate-polyacrylamide gel and electroblotted onto a polyvinylidene difluoride filter. The PrP was detected

using a monoclonal antibody, SAF83 (1:5000; SPI-Bio, Massy, France), followed by an alkaline phosphatase-conjugated goat anti-mouse antibody (1:20,000; Promega Corp., Madison, WI). Immunoreactivity was visualized using a CDP-Star detection reagent (Amersham, Piscataway, NJ). More than three independent assays were performed in each experiment.

The cell surface level of cellular PrP was assayed using flow cytometry, as described previously (10). Briefly, N2a cells dispersed by treatment with 0.1% collagenase (Wako Pure Chemical Industries Ltd., Osaka, Japan) were washed with ice-cold 0.5% fetal calf serum in PBS and incubated with SAF83 (1:500) or isotype-matched control immunoglobulin G1 for 20 min on ice. Cells were washed with 0.5% fetal calf serum in PBS and incubated with goat F(ab')2 fragment anti-mouse immunoglobulin G (heavy plus light chain)-phycoerythrin (1:100) (Beckman Coulter Inc., CA) for 20 min on ice. After washing, cells were analyzed using an EPICS XL-ADC flow cytometer (Beckman Coulter Inc., CA).

Pharmacokinetic studies. Brain cpd-B levels in the animals were assayed as described previously (20) after a 1-week feeding with 0.2% cpd-B ad libitum. All animals were sacrificed at 9:00 a.m. of day 8 by excision of the carotid artery under deep ether anesthesia to remove as much blood as possible, and the brain was collected, rinsed with saline, and weighed. Because preliminary studies found no significant difference in the data for perfused brains and nonperfused brains, the brain was not perfused with saline to remove residual blood. The brain was homogenized with 2 ml of 100% methanol for mouse brain or 4 ml for hamster brain. After centrifugation of the homogenate at 800 × *g* for 10 min, the supernatant was diluted with 9 volumes of 20 mM phosphate buffer, pH 6.5 (PB), and then filtered to obtain the sample for analysis. The sample was then applied to a conditioned C_{18} solid-phase extraction cartridge. The compound was eluted with methanol and was diluted with an equal volume of PB. The compound then was separated by high-performance liquid chromatography using a reversed-phase column (C_4, 4.6 × 150 mm; Phenomenex Inc., Torrance, CA). The compound was detected using a UV detector at 285 nm, and the dose of cpd-B per gram of brain tissue was determined.

The kinetics of brain uptake and washout of cpd-B were also investigated as described previously (20). The compound was solubilized in 5% Tween 80 in ethanol and then prepared as a 0.2-mg/ml solution containing 5% Tween 80 and 5% ethanol in saline. The compound at a dose of 1.0 mg/kg of body weight was administered intravenously to ICR mice under ether anesthesia. Both Tween 80 and ethanol are FDA-approved solubilizers of lipophilic medicinal chemicals. At the dose used in the study, neither solubilizer has been reported to cause any toxicity or to affect the pharmacokinetics. At 2 min or 30 min after injection, the blood was collected from the heart using heparin, and then the brain was obtained as described above. The blood plasma was mixed with 3 volumes of acetonitrile and centrifuged at 10,000 × *g* for 5 min. The supernatant was mixed with the same volume of PB and subsequently filtered to obtain the plasma sample for analysis. The preparation for the brain sample for analysis and the assay of the samples were performed as described above. The percentage of the injected dose per gram of tissue or fluid was used as a measure of the brain or plasma level of the compound.

In vivo treatment in animal models. In experimental animals that had been infected intracerebrally with a prion pathogen, cpd-B was given orally ad libitum as a mixture with powder feed at doses of 0.1%, 0.13%, 0.2%, and 0.33% by weight in the feed, corresponding, respectively, to ca. 150 mg/kg of body weight/day, ca. 225 mg/kg of body weight/day, ca. 300 mg/kg of body weight/day, and ca. 500 mg/kg of body weight/day in Tga20 mice, as each mouse consumed an average of 3.75 g of the feed per day. The animals were monitored every day until the terminal stage of disease; the incubation period, which was defined in the present study as the length of time from inoculation to the terminal stage of disease, was determined.

Pathological and infectivity assays. The right brain hemispheres of the mice were fixed using 10% buffered formalin and then embedded in paraffin. Three-micrometer-thick sections of the coronal slice sited at around one-third of the distance from the interaural line to the bregma line were dewaxed and immunostained using an anti-PrP-C antibody, as described above, or an antibody against glial fibrillary acidic protein (1:5,000; Dako, Glostrup, Denmark), as described in a previous study (9).

For detection of PrPres by immunoblotting, the left brain hemisphere was homogenized with 9 volumes of lysis buffer; after low-speed centrifugation, the supernatant was treated with 50 μg/ml proteinase K for 30 min at 37°C. An aliquot corresponding to 0.13 mg of brain tissue for PrPres assay or 0.83 μg of brain tissue for total PrP assay was electrophoresed on a 13.5% Tris-glycine–sodium dodecyl sulfate-polyacrylamide gel and analyzed by immunoblotting as described above.

For the infectivity assay, the left brain hemisphere was homogenized with PBS to produce a 10% brain homogenate. Serially diluted homogenate samples for assay were produced by diluting the brain homogenate serially with 10% brain homogenate of noninfected mice fed with 0.2% cpd-B for 1 month. A 20-μl aliquot of each sample was then inoculated intracerebrally into each of the Tga20 mice. Incubation times were assayed as described above.

Statistical analysis. Statistical significance was analyzed using the Kruskal-Wallis test followed by Scheffè's *F* test for multiple comparisons. Correlation analysis was performed using Spearman's rank correlation coefficient method. The regression coefficient was determined using simple linear regression analysis. The survival rate was calculated using the Kaplan-Meier method; its significance was evaluated using the log rank method.

RESULTS

Antiprion activity in vitro. The antiprion activities of newly synthesized compounds were investigated using ScN2a cells, which are N2a cells that are persistently infected with RML scrapie prion and are commonly used for drug screening. At a half-maximum effective concentration (EC_{50}) of about 60 pM, cpd-B inhibited PrPres formation (Table 1 and Fig. 1A). Other related compounds were also potent within a nontoxic dose range of up to 10 μM.

To investigate whether the efficacies of the compounds depend on the pathogen strain, cpd-B was tested in four other cell lines that had been infected individually with distinct prion strains. As shown in Fig. 1A, cpd-B was effective only in N002 (EC_{50}, 320 nM) and Ch2 (EC_{50}, 300 nM), both of which are N2a-58 cells infected with RML prion. However, the inhibitory activity in these cells was not as strong as that in ScN2a cells, which are derived from N2a cells expressing one-fifth of the normal PrP molecules of N2a-58 cells. In contrast, cpd-B was ineffective in both N167 cells (N2a cells infected with 22L scrapie prion) and F3 cells (N2a-58 cells infected with Fukuoka-1 GSS prion) at a dose of less than 10 μM. However, at a dose of 10 μM, a marginal reduction of the PrPres signals was observed in both cells. At a dose of greater than 10 μM, cell toxicity was observed. The results suggest that cpd-B exerts an inhibitory activity on PrPres formation in a prion strain-dependent manner: more effectively for RML prion and marginally for 22L prion or Fukuoka-1 prion.

The inhibition mechanism included no alteration of either the total or the cell surface level of normal PrP, as demonstrated in noninfected N2a cells treated with 1 μM cpd-B, using either immunoblot analysis of the cell lysate without protease digestion or flow cytometry analysis of the cell surface PrP (Fig. 1B and C). In addition, cpd-B did not facilitate the digestion of abnormal PrP by proteinase K, nor did it interfere with immunodetection, because PrPres signals were not modified after cpd-B was mixed and incubated with a cell lysate of nontreated ScN2a cells before proteinase K digestion (data not shown).

Pharmacological properties. Abnormal PrP amyloid imaging by cpd-B was performed on brain sections of GSS cases to examine the amyloidophilic properties of cpd-B. The compound bound to and fluorescently labeled most of the PrP plaques in cerebellar cortices of GSS cases (Fig. 1D). Background staining was barely observed after rinsing off the excess compound. Immunohistochemical analysis of PrP revealed that the compound achieved high-specificity labeling. The compound displayed no signal in control sections without amyloid lesions (data not shown).

Next, to examine the brain accessibility of cpd-B when administered orally, brain levels of cpd-B in the experimental

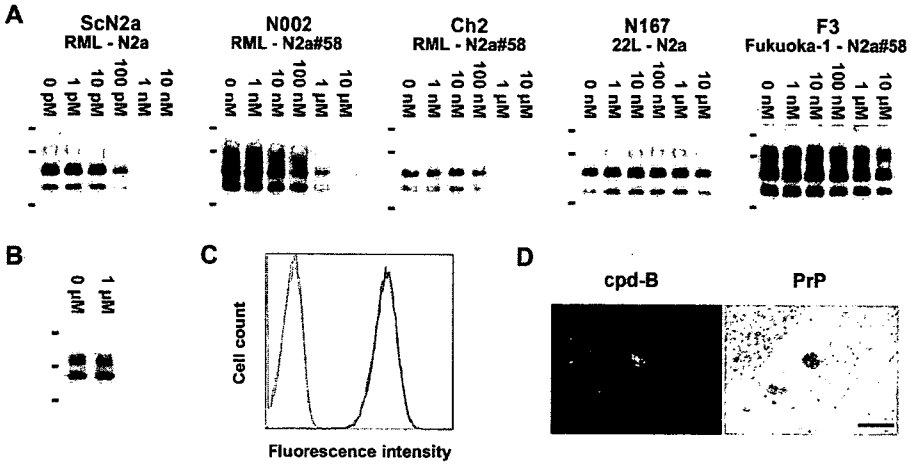

FIG. 1. cpd-B effects on prion-infected and noninfected cells and its amyloidophilic property. (A) Immunoblot analyses of PrPres formation in various prion-infected cells treated with the indicated concentrations of cpd-B. N2a-58 (N2a#58) is a stable transformant of N2a and expresses five-times-higher levels of PrP than N2a. Ch2 is a subclone of N002. The bars on the left are molecular size markers for 41, 32, and 18 kDa. (B) Immunoblot analysis of total normal PrP in noninfected N2a cells treated with cpd-B. Molecular size markers on the left are 47, 32, and 25 kDa. (C) Flow cytometric analysis of cell surface-normal PrP in noninfected N2a cells treated with 1 μM cpd-B. The solid and broken lines, respectively, indicate cpd-B-treated cells and nontreated cells. Gray line peaks on the left show their respective controls, using isotype immunoglobulin as a first antibody. (D) Imaging of abnormal PrP plaques in the brain tissue by cpd-B. Abnormal PrP deposition in a cerebellar tissue from a case of GSS was fluorescently labeled with cpd-B and subsequently immunostained with an anti-PrP antibody. Bar, 50 μm.

animals used in the study were assayed after the animals were fed ad libitum with 0.2% cpd-B-containing feed for 1 week. The brain level of cpd-B was 39.16 ± 22.15 nmol/g brain tissue in Tga20 mice (n = 4), 26.04 ± 12.50 nmol/g brain tissue in ICR mice (n = 4), and 22.94 ± 7.64 nmol/g brain tissue in Tg7 mice (n = 4). Syrian hamsters, however, showed a lower level, 7.26 ± 2.47 nmol/g brain tissue (n = 4). A considerable amount of cpd-B was detected in the brains of all experimental animals; no significant difference in the brain cpd-B levels was found among the types of the mice.

Further study of the pharmacokinetics of cpd-B in the blood and the brain was performed with ICR mice after cpd-B was injected into the tail vein. The percentage of the injected dose per gram of tissue or fluid was determined. The brain uptake level of cpd-B at 2 min after intravenous injection was 8.01% ± 1.27% of the injected dose/g tissue, whereas the blood plasma level was 2.92% ± 1.00%/g fluid. Consequently, the ratio of the cpd-B concentration in the brain to that in the blood plasma is 2.7:1, indicating that cpd-B is equal to the best brain-entering amyloidophilic chemicals previously identified (15). On the other hand, both the brain level and the blood plasma level of cpd-B at 30 min after the intravenous injection were below the measurable level of 50 pM, which indicates that cpd-B is very rapidly washed out from the brain and blood.

Regarding toxicity of cpd-B, body weight losses of about 16% in Tga20 mice and about 5% in Tg7 mice were observed after cpd-B was given orally ad libitum for 1 week at a dose of 0.33% weight in feed, which corresponds to ca. 500 mg/kg of body weight/day. Other doses of cpd-B tested in this study produced no apparent toxic effects in the experimental animals used.

Therapeutic efficacy in vivo. The therapeutic activity of cpd-B in vivo was assayed in murine PrP-overexpressing Tga20 mice that had been cerebrally infected with RML scrapie prion. The nontreated infected mice started exhibiting abnormal clinical signs such as staggering, rotating, irritation, and motionlessness at about 2 months after the infection; the mice then wasted into the terminal stage of disease in a week. Treatment by feeding cpd-B-containing feed ad libitum was initiated immediately after the infection and continued until the terminal stage of disease. The cpd-B-treated mice did not exhibit such abnormal signs as described above and wasted gradually into the terminal stage of disease. As shown in Fig. 2A, oral cpd-B treatment significantly prolonged the incubation periods of infected Tga20 mice in a dose-dependent manner; these were 68.5 ± 5.9 days in the nontreated control mice, 108.0 ± 2.8 days in the mice treated with 0.1% cpd-B feed, 120.5 ± 10.7 days in the mice with 0.13% cpd-B feed, and 154.3 ± 19.9 days in the mice with 0.2% cpd-B feed. Therefore, oral cpd-B treatment at the highest dose produced a 2.3-fold extension of the incubation periods of the mice. Statistical analyses demonstrated a significant linear correlation between the incubation periods and the cpd-B doses (r = 0.95; $P < 0.01$); the correlation equation was $y = 426.37x + 66.93$ (y, incubation period [days]; x, cpd-B dose [percentage in feed]), and the correlation coefficient was 0.89 ($P < 0.01$).

In our previous studies, the effectiveness of amyloidophilic chemicals in the extension of incubation periods of infected animals was observed only in Tga20 mice infected with RML prion (14, 15). ICR mice were then examined for the therapeutic efficacy of oral cpd-B treatment to investigate whether effectiveness of amyloidophilic compounds is restricted only to Tga20 mice. Nontreated control ICR mice that had been cerebrally infected with RML prion were in the terminal stage of disease at 154.2 ± 18.4 days postinfection, whereas the mice treated with 0.2% cpd-B feed lived significantly longer ($P < 0.01$). Even though the oral cpd-B treatment was discontinued at day 187 postinfection when the last of the nontreated animals reached the terminal stage of disease, more than half of the treated mice survived to day 270 postinfection (Fig. 2B).

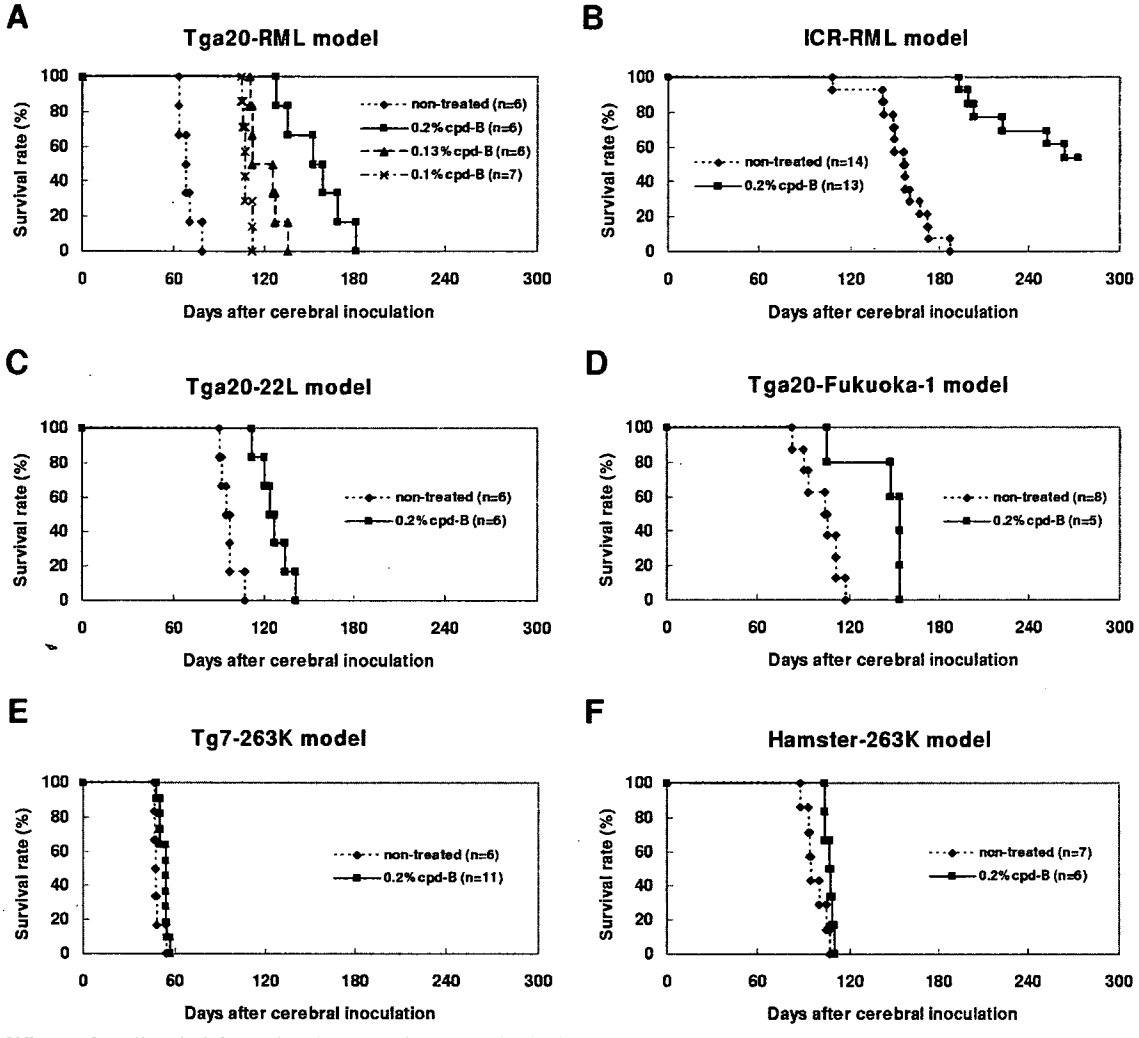

FIG. 2. Effects of orally administered cpd-B on animals cerebrally infected with prion diseases. cpd-B was given orally in a mixed form with powder feed ad libitum throughout the incubation periods in all animal disease models except the ICR-RML model, in which oral cdp-B treatment was discontinued at the time when the last of the nontreated animals reached the terminal stage of disease. In this study, the incubation periods are defined as the periods from the cerebral infection to the terminal stage of disease. Survival rates were calculated using the incubation periods and are plotted using the Kaplan-Meier method.

Next, the therapeutic efficacy of oral cpd-B treatment against other prion strains was investigated. The cpd-B treatment significantly prolonged the incubation periods of Tga20 mice that had been cerebrally infected with 22L scrapie prion ($P < 0.01$); these were 96.3 ± 5.9 days in the nontreated control mice and 126.3 ± 10.3 days in the mice treated with 0.2% cpd-B feed, indicating a 1.3-fold extension of the incubation period (Fig. 2C). Control mice started exhibiting distinguished opisthotonus with head rotating a week before the terminal stage of disease, whereas cpd-B treated mice showed no such clinical sign, even in the terminal stage.

cpd-B was also effective against Fukuoka-1 GSS prion. Cerebrally infected Tga20 mice lived significantly longer with oral cpd-B treatment ($P < 0.05$), i.e., 101.6 ± 12.1 days for the nontreated control mice and 142.2 ± 21.0 days for the mice treated with 0.2% cpd-B feed, indicating a 1.4-fold extension of the incubation period (Fig. 2D). Staggering was observed as an initial clinical sign in the control mice more than 1 week before the terminal stage of disease, although this clinical sign was not seen in the cpd-B treated mice.

In contrast to the case for these prion strains, the efficacy of oral cpd-B treatment was very marginal for 263K scrapie prion when Tg7 mice expressing hamster PrP were used as the host (Fig. 2E). The incubation periods of the cpd-B-treated mice (52.7 ± 2.8 days) were significantly but very marginally longer than those of the nontreated mice (48.0 ± 3.0 days) ($P < 0.05$). This prion is a hamster-adapted scrapie prion strain; Syrian hamsters were used as the host to examine whether the marginal efficacy of oral cpd-B treatment is attributable chiefly to the host Tg7 mouse or to the pathogen strain 263K prion. As observed in Tg7 mice, hamsters treated with 0.2% cpd-B feed also exhibited a marginal increase in the incubation period compared to that of the nontreated control hamsters that had been cerebrally infected with 263K prion ($P < 0.05$): 107.0 ± 2.5 days in the cpd-B treated hamsters and 97.4 ± 6.9 days in the non-

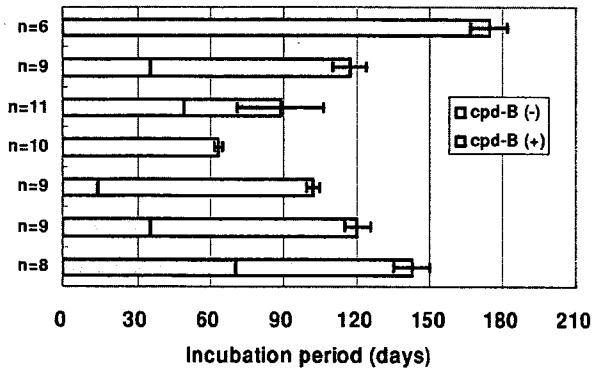

FIG. 3. cpd-B effects throughout various timings and durations of oral administration. Tga20 mice cerebrally infected with RML prion were treated with 0.2% cpd-B feed at different times and for different durations, and the incubation periods were assayed. Open bars indicate the durations of no treatment [cpd-B (−)]. Shaded bars indicate the durations of oral cpd-B treatment [cpd-B (+)].

treated hamsters (Fig. 2F). These results indicate that oral cpd-B treatment is not as effective for 263K prion.

Timing and duration of dosing. The effectiveness of cpd-B at various timings and durations of oral administration was analyzed in Tga20 mice that had been cerebrally infected with RML prion (Fig. 3). The incubation periods of the nontreated mice were 63.0 ± 1.8 days, whereas the incubation periods of the mice treated with 0.2% cpd-B feed were inversely correlated with the postinfection durations to the commencement of cpd-B treatment ($r = -0.79$; $P < 0.01$): 174.5 ± 7.6 days when started at day 0 postinfection, 117.2 ± 7.0 days when started at day 35 postinfection, and 88.7 ± 17.3 days when started at day 49 postinfection. On the other hand, the incubation periods of the mice treated with 0.2% cpd-B feed were also correlated with the durations of cpd-B treatment which started immediately after cerebral infection ($r = 0.95$, $P < 0.01$): 102.1 ± 2.9 days when treated for 14 days from the infection, 120.2 ± 5.2 days when treated for 35 days from the infection, and 142.5 ± 7.8 days when treated for 70 days from the infection. In addition, when the cpd-B treatment was discontinued during early disease stages, the remaining incubation times were longer than that of the control mice.

Pathological evaluation. The PrPres content in the brains of cpd-B-treated mice was analyzed sequentially by immunoblotting and compared with that in the nontreated control mice (Fig. 4A). The PrPres signals in the nontreated mice were very strong at the terminal stage of disease (day 63 postinfection). In contrast, in the mice treated with 0.1% cpd-B feed from the start of infection, PrPres signals were faint at day 63 postinfection and distinct at the terminal stage of disease (day 108 postinfection). However, the PrPres signals at the terminal stage of disease did not reach the high level shown by the nontreated control mice at that stage. Comparison of the signal intensities of the diglycosylated PrPres form showed that 6- to 15-fold-diluted samples from the nontreated terminal mice exhibited signal intensities similar to those of undiluted or 2-fold-diluted samples from the 0.1% cpd-B-treated terminal mice (Fig. 4B). Similarly, in the mice treated with 0.2% cpd-B feed from the start of infection, PrPres signals gradually increased according to the time course after infection: no signals were detected at day 63 postinfection, distinct signals were detected at day 120, and similar or more distinct signals were detected at the terminal stage of infection (day 154 postinfection). The PrPres signal levels of the 0.2% cpd-B-treated mice at the terminal stage of disease were indistinguishable from those of the 0.1% cpd-treated mice at the terminal stage of disease.

The glycoform patterns of PrPres differed completely. As shown in Fig. 4B, when the samples were diluted and reassayed so that the signal intensities of diglycosylated PrPres forms were equalized as much as possible, the difference was much more distinct. The glycoform patterns in the nontreated mice, which were uniform in the analyzed samples, were predominantly monoglycosylated, whereas the glycoform patterns in the cpd-B-treated mice were not necessarily uniform but were always predominantly diglycosylated. This predominance of diglycosylated PrPres was also observed for 263K prion (Fig. 4C) but not for other prion strains used in this study (data not shown).

Modification in the pathology of the brains of cpd-B-treated mice was analyzed (Fig. 4D). For nontreated control mice with an incubation period of 63 days, the brain showed prominent pathological changes consisting of abnormal PrP deposition and glial cell reaction in the thalamus, although the brains of the mice treated with 0.2% cpd-B feed showed no such pathological changes at day 63 postinfection and milder levels of abnormal PrP deposition at the terminal stage of disease (day 154 postinfection). No difference was apparent in the pattern or distribution of abnormal PrP deposition in the brains between the nontreated mice and the cpd-B-treated mice.

Infectivity analysis. Infectivity levels are inversely correlated with incubation periods (24). Therefore, infectivity levels of the brains of the mice treated with 0.2% cpd-B feed were evaluated by assaying the incubation periods of animals that had been cerebrally inoculated with the brain homogenate (Table 2). The 10^2-fold-diluted brain homogenates from the cpd-B-treated mice at day 63 postinfection exhibited incubation periods similar to those of the 10^5-fold- or greater diluted brain homogenates from the nontreated mice; the 10^2-fold-diluted brain homogenates from the cpd-B-treated mice at the terminal stage of disease (day 154 postinfection) showed incubation periods similar to those of the 10^4-fold- or 10^5-fold-diluted brain homogenates from the nontreated mice. The data indicate that the brains of mice treated with 0.2% cpd-B feed had much lower infectivity levels than those of the nontreated mice at the same time point after infection and even at the terminal stage of disease. A 100-fold to 1,000-fold difference in infectivity levels was apparent between the nontreated terminal mice and the cpd-B-treated terminal mice, although a less-than-100-fold difference in PrPres levels between the two mouse groups was estimated from the immunoblot data shown in Fig. 4B. On the other hand, no inconsistency was apparent in the gaps in the infectivity levels and the PrPres levels between the cpd-B-treated mice at day 63 postinfection and those at the terminal stage of disease. The gap in infectivity levels between these two groups was around 10-fold; 10-fold dilution of the samples from the cpd-B-treated terminal mice similarly produced no signals on the immunoblot, as observed in the samples from the cpd-B-treated mice at day 63 postinfection (data not shown).

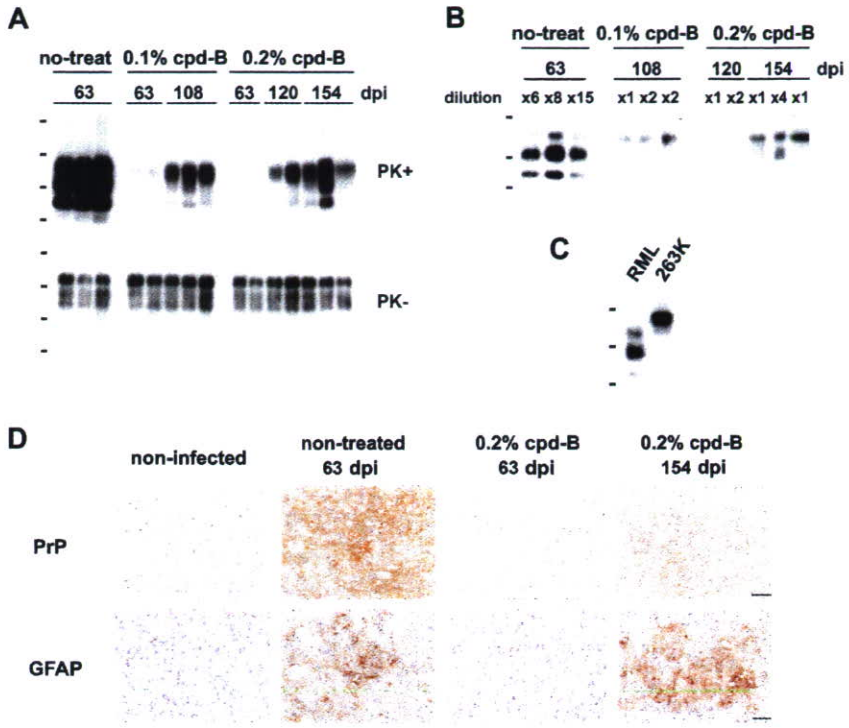

FIG. 4. Immunoblot and immunohistochemical analyses of cpd-B-treated animal brains. (A) Immunoblot analysis of PrP in the brains of nontreated mice (no-treat) or mice treated with 0.1% cpd-B feed or 0.2% cpd-B feed. Each lane represents an aliquot corresponding to 0.13 mg for PrPres (PK+) or 0.83 μg for total PrP (PK−) of brain tissue from each mouse sacrificed at a designated day after cerebral infection (dpi). Molecular size markers on the left show 47, 32, 25, and 16 kDa. (B) Immunoblot analysis of PrPres of some of the samples in panel A, which were diluted and reassayed to equalize signal intensities of the diglycosylated PrPres bands as much as possible for comparison of the signal intensity and the glycoform pattern of PrPres. Molecular size markers on the left show 32, 25, and 16 kDa. (C) Immunoblot analysis of PrPres to compare the glycoform patterns of the RML prion and the 263K prion. Analyzed samples were from an RML prion-infected mouse brain and a 263K prion-infected hamster brain. Molecular size markers on the left are the same as those in panel B. (D) Immunohistochemical analysis of abnormal PrP deposition (PrP) and neurodegenerative changes by means of astrocytic glial reaction (glial fibrillary acidic protein [GFAP]) in the brains of noninfected mice, infected but nontreated mice, and infected mice treated with 0.2% cpd-B feed. Data from each representative mouse sacrificed at a designated day after cerebral infection (dpi) are shown; every picture was taken from an almost identical area of the thalamus. The samples of 0.2% cpd-B at 63 dpi and 0.2% cpd-B at 154 dpi are from the same individual mouse as the samples in the right lane of 0.2% cpd-B 63 dpi and the rightmost lane of 0.2% cpd-B 154 dpi in panel A, respectively. Bar, 50 μm.

DISCUSSION

In this study, the newly synthesized chemical cpd-B was discovered as an orally available antiprion compound that is effective for prolonging the incubation periods of animals cerebrally infected with prion diseases. This compound has no similarity in chemical structure to previously reported antiprion compounds, although the compound shares the following properties with antiprion amyloidophilic chemicals we previously reported, such as (*trans*, *trans*)-1-bromo-2,5-bis-(3-hydroxycarbonyl-4-hydroxy)styrylbenzene and styrylbenzoazole chemicals: binding to PrP amyloid plaques in the brain tissue, inhibiting abnormal PrP formation in prion-infected cells without any effect on either normal PrP expression level or protease sensitivity of abnormal PrPres, preferential antiprion effects in RML prion-infected cells rather than 22L prion-infected or Fukuoka-1 prion-infected cells, and prolonging the incubation period in the RML prion-infected Tga20 mouse model but never or only marginally in the 263K prion-infected Tg7 mouse model. The discovery of orally available cpd-B effectiveness reinforces the idea that amyloidophilic chemicals can serve as one class of antiprion drug candidates.

This study has shown that prion strains are definitely influential in the outcome of the treatment with antiprion compounds. Treatment with cpd-B was effective against all tested prion strains, but both its antiprion effectiveness in vitro and its therapeutic efficacy in vivo were consistently dependent on the prion strain. In fact, cpd-B was most effective against RML prion but less effective against 22L prion and Fukuoka-1 prion either in vitro or in vivo. In addition, its lowest effectiveness in therapeutic efficacy was demonstrated identically in either the 263K prion-infected Tg7 mouse model or the 263K prion-infected hamster model, although its effectiveness against 263K prion could not be evaluated on the same host background as that used for the other prion strains. It is unlikely that differences in the hosts used in this study are influential in the therapeutic efficacy of cpd-B treatment, because the brain chemical levels in all types of mice fed with 0.2% cpd-B for 1 week were not significantly different.

Amyloidophilic chemicals are not the only class of antiprion compound that exhibits the therapeutic efficacy in a prion strain-dependent manner. The polyene antibiotic amphotericin B is another example, but it is opposite to amyloidophilic chemicals and is specifically effective against 263K prion (1).

TABLE 2. Infectivity assays of the brains of nontreated mice or cpd-B-treated mice

Dilution	Nontreated mice (63 dpi[a])			cpd-B treated mice (63 dpi)			cpd-B treated mice (154 dpi)		
	Mouse no.	No. of diseased mice/total	Mean incubation time (days) ± SD	Mouse no.	No. of diseased mice/total	Mean incubation time (days) ± SD	Mouse no.	No. of diseased mice/total	Mean incubation time (days) ± SD
10^2	cnt-1	8/8	77.4 ± 4.5	bc-1[d]	7/7	284.1 ± 54.6	bl-1	7/7	122.0 ± 14.0
				bc-2[e]	8/8	136.8 ± 19.2	bl-2[f]	7/7	92.6 ± 8.9
							bl-3	7/7	89.1 ± 4.0
10^3	cnt-1	8/8	84.4 ± 6.9	bc-1[d]	0/7	>140[c]	bl-1	5/9	>140[c]
	cnt-2	6/6	75.3 ± 2.4	bc-2[e]	1/8	>140[c]	bl-2[f]	7/7	97.4 ± 9.6
	cnt-3	7/7	75.7 ± 7.4				bl-3	9/9	101.6 ± 7.4
10^4	cnt-1	7/7	88.4 ± 7.3	bc-1[d]	1/8	>140[c]	bl-1	1/9	>140[c]
				bc-2[e]	1/9	>140[c]	bl-2[f]	3/7	>140[c]
							bl-3	3/7	>140[c]
10^5	cnt-1	6/6	155.7 ± 55.3						
	cnt-2	7/7	105.4 ± 16.5						
	cnt-3	7/7	95.9 ± 7.1						
10^6	cnt-1	1/7	>420[b]						
10^7	cnt-1	3/7	>420[b]						
10^8	cnt-1	1/7	>420[b]						
10^9	cnt-1	2/7	>420[b]						

[a] Days after cerebral inoculation.
[b] Observed up to 420 days postinoculation.
[c] Observed up to 140 days postinoculation.
[d] Mouse for the sample in the left lane of 0.2% cpd-B at 63 dpi in Fig. 4A.
[e] Mouse for the sample in the right lane of 0.2% cpd-B at 63 dpi in Fig. 4A.
[f] Mouse for the sample of the rightmost lane of 0.2% cpd-B at 154 dpi in Fig. 4A.

Either variation in strain-specific PrP conformational structures or variation in microenvironments facilitating PrP conformational changes might be involved in the mechanism of prion strain-dependent efficacy. The results of this study showed that prions producing predominantly diglycosylated PrPres molecules were least sensitive or resistant to cpd-B treatment, which suggests that either the conformational structure responsible for PrPres or the diglycosylation moieties might affect the interaction of the compound with abnormal PrP molecules, although this inference must be examined further. The findings indicate that each class of antiprion compounds must be examined using various prion strains to learn more about prion strain dependency.

Even in the terminal stage of disease, both abnormal PrP deposition levels in the brain and infectivity levels in the brain were reduced in the mice treated with cpd-B compared to the nontreated control mice. It remains unclear why this gap occurs. One possibility is that the treated mice prematurely fell into the terminal stage because of accumulated cpd-B toxicity. This inference, however, does not seem to be correct, because the noninfected mice treated with 0.2% cpd-B feed for more than 1 year showed no clinical signs and appeared healthy. Another possibility is that neuronal cells in the brain might be more vulnerable to lower levels of abnormal PrP in the presence of cpd-B or that abnormal PrP bound with cpd-B might be more toxic to the neuronal cells in the brain. However, these inferences also seem to be unlikely, because the toxicity of PrP106-126 peptide amyloid, which is reminiscent of abnormal PrP, in primary neuronal cell cultures is attenuated by the presence of cpd-B (unpublished data). Another possibility is that prion strains modified or selected from the original by the compound might multiply in the animals and cause the disease; this inference is supported by data showing that PrPres molecules with different glycoform patterns were detected in the treated mice. Further study, however, must provide evidence to support this inference. The findings indicate that life-threatening levels of either infectivity or abnormal PrP in the brain are not necessarily the same between treated animals and nontreated animals.

A large quantity of cpd-B was needed for efficacy in vivo; disease progression was not halted even though the treatment commenced immediately after the infection and continued to the terminal stage of disease. This limited effectiveness of cpd-B might be partly attributable to the pharmacological properties of its rapid washout from either the brain or the blood, because it is assumed that the compounds with better brain permeativity and longer retention in the brain might produce more beneficial results in prion-infected animals. In addition, some metabolic instability of the compound might be responsible for its limited effectiveness, especially the loss of efficacy during long-term administration. In fact, cpd-B is easily metabolized in the presence of mouse liver microsome extracts (unpublished data). Therefore, the pharmacokinetic parameters of this compound must be improved for better efficacy.

The effectiveness of cpd-B is dependent upon the timing and duration of administration; an earlier start of administration is

necessary to maximize beneficial results. Therefore, diagnostic measures in much earlier disease stages, especially presymptomatic stages, are vital to produce more beneficial outcomes. In addition, multidrug combination chemotherapy using several antiprion compounds with different actions might produce more beneficial results. This study suggests that cpd-B inhibits new formation of abnormal PrP but does not facilitate the degradation of already formed abnormal PrP, because a mixture of cpd-B with abnormal PrP did not modify the protease-resistant property of abnormal PrP. In addition, cpd-B itself has no activity to protect neuronal cells from neurotoxic insults aside from PrP amyloid (unpublished data), suggesting that cpd-B does not protect neuronal cells from neurodegenerative insults that are induced secondarily by abnormal PrP. Combinations of cpd-B with other compounds such as doxycycline, flupirtine, and simvastatin might be examples, but their efficacy must be evaluated. Doxycycline is a tetracycline antibiotic known to destabilize abnormal PrP (12). Flupirtine is a centrally acting nonopioid analgesic and protects neuronal cells from apoptotic cell death induced by toxic PrP106-126 peptide amyloid (29). It was used in clinical trials, where beneficial effects on cognitive functions in patients with CJD were proved (21). Simvastatin is a cholesterol-lowering drug known to prevent abnormal PrP formation in prion-infected cells, presumably by redistribution of normal PrP away from cholesterol-rich lipid rafts (13, 31). It prolongs survival times in prion-infected animals (16, 17).

Recently, long-term cerebroventricular administration of pentosan polysulfate (PPS), a clinical approach based on our preclinical study in rodent models of prion diseases (9), has been carried out in 26 patients with various types of diseases (27). Although its therapeutic efficacy remains to be confirmed, preliminary clinical experience indicates prolonged survival in some patients receiving long-term PPS (22, 27). Further prospective investigation of PPS administration is necessary to obtain high-quality evidence for its clinical benefits. However, this treatment has some weaknesses. One is the requirement for surgical implantation of a continuous infusion pump and an intraventricular catheter, which could become an obstacle to extension of clinical trials because of the potential risks of prion contamination in operating rooms and of operation instruments, although most developed countries now possess clearly defined and well established guidelines for safe surgical and anesthetic management of patients with prion diseases. Compared to such treatments, the treatments using orally available antiprion compounds are absolutely preferable and practical.

The compounds tested in the study were originally designed as therapeutic lead chemicals for the treatment of Alzheimer's disease. In fact, cpd-B and related chemicals are very effective in vitro in either inhibiting beta-amyloid formation or protecting neuronal cells from beta-amyloid toxicity; in addition, cpd-B has therapeutic efficacy in an Alzheimer's disease mouse model (unpublished data). Therefore, cpd-B is a therapeutic candidate not only for prion diseases but also for Alzheimer's disease. The search for and development of drugs for prion diseases reportedly do not interest pharmaceutical companies because of the limited number of patients, but the possible use of amyloidophilic chemicals as drug candidates for both prion diseases and Alzheimer's disease might attract and accelerate the development of therapeutic drugs for prion diseases.

In conclusion, our findings related to the newly synthesized amyloidophilic chemical cpd-B are encouraging, but further improvement of its safety profiles and pharmacokinetic properties is necessary before clinical application can be considered. Moreover, additional problems exist with its prion strain-dependent effectiveness and with its reduced effectiveness if administered at later disease stages.

ACKNOWLEDGMENTS

This work was supported by grants from the Japanese Ministry of Health, Labor and Welfare (H16-kokoro-024 and H19-nanji-006); the Japanese Ministry of Agriculture, Forestry and Fisheries; and the Japan Society for the Promotion of Science (A2-14207030 and B-19390234).

We thank Kayoko Motoki, Takashi Odagiri, and Tetsuya Mimura from Daiichi Pharmaceutical Co., Ltd., for synthesis of the amyloidophilic compounds tested in the study; Yuki Yamada and Hiroto Akama from Tohoku University for technical assistance; and Tetsuyuki Kitamoto and Yukitsuka Kudo from Tohoku University for helpful suggestions.

REFERENCES

1. **Adjou, K. T., J. P. Deslys, R. Demaimay, and D. Dormont.** 1997. Probing the dynamics of prion diseases with amphotericin B. Trends Microbiol. **5**:27–31.
2. **Bresjanac, M., L. M. Smid, T. D. Vovko, A. Petric, J. R. Barrio, and M. Popovic.** 2003. Molecular-imaging probe 2-(1-[6-[(2-fluoroethyl)(methyl)-amino]-2-naphthyl]ethylidene)malononitrile labels prion plaques in vitro. J. Neurosci. **23**:8029–8033.
3. **Cai, L., R. B. Innis, and V. W. Pike.** 2007. Radioligand development for PET imaging of beta-amyloid (Abeta)—current status. Curr. Med. Chem. **14**: 19–52.
4. **Cashman, N. R., and B. Caughey.** 2004. Prion diseases—close to effective therapy? Nat. Rev. Drug Discov. **3**:874–884.
5. **Caughey, B., and R. E. Race.** 1992. Potent inhibition of scrapie-associated PrP accumulation by Congo red. J. Neurochem. **59**:768–771.
6. **Caughey, B., and G. J. Raymond.** 1993. Sulfated polyanion inhibition of scrapie-associated PrP accumulation in cultured cells. J. Virol. **67**:643–650.
7. **Doh-ura, K., E. Mekada, K. Ogomori, and T. Iwaki.** 2000. Enhanced CD9 expression in the mouse and human brains infected with transmissible spongiform encephalopathies. J. Neuropathol. Exp. Neurol. **59**:774–785.
8. **Doh-Ura, K., T. Iwaki, and B. Caughey.** 2000. Lysosomotropic agents and cysteine protease inhibitors inhibit scrapie-associated prion protein accumulation. J. Virol. **74**:4894–4897.
9. **Doh-ura, K., K. Ishikawa, I. Murakami-Kubo, K. Sasaki, S. Mohri, R. Race, and T. Iwaki.** 2004. Treatment of transmissible spongiform encephalopathy by intraventricular drug infusion in animal models. J. Virol. **78**:4999–5006.
10. **Doh-Ura, K., T. Kuge, M. Uomoto, K. Nishizawa, Y. Kawasaki, and M. Iha.** 2007. Prophylactic effect of dietary seaweed fucoidan against enteral prion infection. Antimicrob. Agents Chemother. **51**:2274–2277.
11. **Fischer, M., T. Rulicke, A. Raeber, A. Sailer, M. Moser, B. Oesch, S. Brandner, A. Aguzzi, and C. Weissmann.** 1996. Prion protein (PrP) with amino-proximal deletions restoring susceptibility of PrP knockout mice to scrapie. EMBO J. **15**:1255–1264.
12. **Forloni, G., S. Iussich, T. Awan, L. Colombo, N. Angeretti, L. Girola, I. Bertani, G. Poli, M. Caramelli, M. Grazia Bruzzone, L. Farina, L. Limido, G. Rossi, G. Giaccone, J. W. Ironside, O. Bugiani, M. Salmona, and F. Tagliavini.** 2002. Tetracyclines affect prion infectivity. Proc. Natl. Acad. Sci. USA **99**:10849–10854.
13. **Gilch, S., C. Kehler, and H. M. Schatzl.** 2006. The prion protein requires cholesterol for cell surface localization. Mol. Cell Neurosci. **31**:346–353.
14. **Ishikawa, K., K. Doh-ura, Y. Kudo, N. Nishida, I. Murakami-Kubo, Y. Ando, T. Sawada, and T. Iwaki.** 2004. Amyloid imaging probes are useful for detection of prion plaques and treatment of transmissible spongiform encephalopathies. J. Gen. Virol. **85**:1785–1790.
15. **Ishikawa, K., Y. Kudo, N. Nishida, T. Suemoto, T. Sawada, T. Iwaki, and K. Doh-ura.** 2006. Styrylbenzoazole derivatives for imaging of prion plaques and treatment of transmissible spongiform encephalopathies. J. Neurochem. **99**:198–205.
16. **Kempster, S., C. Bate, and A. Williams.** 2007. Simvastatin treatment prolongs the survival of scrapie-infected mice. Neuroreport **18**:479–482.
17. **Mok, S. W., K. M. Thelen, C. Riemer, T. Bamme, S. Gultner, D. Lutjohann, and M. Baier.** 2006. Simvastatin prolongs survival times in prion infections of the central nervous system. Biochem. Biophys. Res. Commun. **348**:697–702.
18. **Murakami-Kubo, I., K. Doh-Ura, K. Ishikawa, S. Kawatake, K. Sasaki, J.**

Kira, S. Ohta, and T. Iwaki. 2004. Quinoline derivatives are therapeutic candidates for transmissible spongiform encephalopathies. J. Virol. **78**:1281–1288.

19. **Okamura, N., T. Suemoto, H. Shimadzu, M. Suzuki, T. Shiomitsu, H. Akatsu, T. Yamamoto, M. Staufenbiel, K. Yanai, H. Arai, H. Sasaki, Y. Kudo, and T. Sawada.** 2004. Styrylbenzoxazole derivatives for in vivo imaging of amyloid plaques in the brain. J. Neurosci. **24**:2535–2541.
20. **Okamura, N., T. Suemoto, S. Furumoto, M. Suzuki, H. Shimadzu, H. Akatsu, T. Yamamoto, H. Fujiwara, M. Nemoto, M. Maruyama, H. Arai, K. Yanai, T. Sawada, and Y. Kudo.** 2005. Quinoline and benzimidazole derivatives: candidate probes for in vivo imaging of tau pathology in Alzheimer's disease. J. Neurosci. **25**:10857–10862.
21. **Otto, M., L. Cepek, P. Ratzka, S. Doehlinger, I. Boekhoff, J. Wiltfang, E. Irle, G. Pergande, B. Ellers-Lenz, O. Windl, H. A. Kretzschmar, S. Poser, and H. Prange.** 2004. Efficacy of flupirtine on cognitive function in patients with CJD: a double-blind study. Neurology **62**:714–718.
22. **Parry, A., I. Baker, R. Stacey, and S. Wimalaratna.** 2007. Long term survival in a patient with variant Creutzfeldt-Jakob disease treated with intraventricular pentosan polysulphate. J. Neurol. Neurosurg. Psychiatry **78**:733–734.
23. **Prusiner, S. B., M. P. McKinley, K. A. Bowman, D. C. Bolton, P. E. Bendheim, D. F. Groth, and G. G. Glenner.** 1983. Scrapie prions aggregate to form amyloid-like birefringent rods. Cell **35**:349–358.
24. **Prusiner, S. B.** 1991. Molecular biology of prion diseases. Science **252**:1515–1522.
25. **Race, R. E., B. Caughey, K. Graham, D. Ernst, and B. Chesebro.** 1988. Analyses of frequency of infection, specific infectivity, and prion protein biosynthesis in scrapie-infected neuroblastoma cell clones. J. Virol. **62**:2845–2849.
26. **Race, R. E., S. A. Priola, R. A. Bessen, D. Ernst, J. Dockter, G. F. Rall, L. Mucke, B. Chesebro, and M. B. Oldstone.** 1995. Neuron-specific expression of a hamster prion protein minigene in transgenic mice induces susceptibility to hamster scrapie agent. Neuron **15**:1183–1191.
27. **Rainov, N. G., Y. Tsuboi, P. Krolak-Salmon, A. Vighetto, and K. Doh-Ura.** 2007. Experimental treatments for human transmissible spongiform encephalopathies: is there a role for pentosan polysulfate? Expert Opin. Biol. Ther. **7**:713–726.
28. **Sadowski, M., J. Pankiewicz, H. Scholtzova, J. Tsai, Y. Li, R. I. Carp, H. C. Meeker, P. Gambetti, M. Debnath, C. A. Mathis, L. Shao, W. B. Gan, W. E. Klunk, and T. Wisniewski.** 2004. Targeting prion amyloid deposits in vivo. J. Neuropathol. Exp. Neurol. **63**:775–784.
29. **Schroder, H. C., and W. E. Muller.** 2002. Neuroprotective effect of flupirtine in prion disease. Drugs Today **38**:49–58.
30. **Smid, L. M., T. D. Vovko, M. Popovic, A. Petric, V. Kepe, J. R. Barrio, G. Vidmar, and M. Bresjanac.** 2006. The 2,6-disubstituted naphthalene derivative FDDNP labeling reliably predicts Congo red birefringence of protein deposits in brain sections of selected human neurodegenerative diseases. Brain Pathol. **16**:124–130.
31. **Taraboulos, A., M. Scott, A. Semenov, D. Avrahami, L. Laszlo, and S. B. Prusiner.** 1995. Cholesterol depletion and modification of COOH-terminal targeting sequence of the prion protein inhibit formation of the scrapie isoform. J. Cell Biol. **129**:121–132.
32. **Trevitt, C. R., and J. Collinge.** 2006. A systematic review of prion therapeutics in experimental models. Brain **129**:2241–2265.

J Neurol (2007) 254:1509–1517
DOI 10.1007/s00415-007-0540-9

ORIGINAL COMMUNICATION

Two different clinical phenotypes of Creutzfeldt-Jakob disease with a M232R substitution

Yusei Shiga
Katsuya Satoh
Tetsuyuki Kitamoto
Sigenori Kanno
Ichiro Nakashima
Shigeru Sato
Kazuo Fujihara
Hiroshi Takata
Keigo Nobukuni
Shigetoshi Kuroda
Hiroki Takano
Yoshitaka Umeda
Hidehiko Konno
Kunihiko Nagasato
Akira Satoh
Yoshito Matsuda
Mitsuru Hidaka
Hirokatsu Takahashi
Yasuteru Sano
Kang Kim
Takashi Konishi
Katsumi Doh-ura
Takeshi Sato
Kensuke Sasaki
Yoshikazu Nakamura
Masahito Yamada
Hidehiro Mizusawa
Yasuto Itoyama

Received: 28 June 2006
Received in revised form: 8 January 2007
Accepted: 6 February 2007
Published online: 2 November 2007

Y. Shiga, MD, PhD* (✉) · S. Kanno, MD · I. Nakashima, MD, PhD · K. Fujihara, MD, PhD · Y. Itoyama, MD, PhD
Dept. of Neurology
Tohoku University Graduate School of Medicine
1-1 Seiryo-machi, Aoba-ku
Sendai 980-8574, Japan
Tel.: +81-22/717-7189
Fax: +81-22/717-7192
E-Mail:
yshiga@em.neurol.med.tohoku.ac.jp

K. Satoh, MD, PhD
The First Department of Internal Medicine
Graduate School of Medicine
Nagasaki University, Japan

T. Kitamoto, MD, PhD*
Division of CJD Science and Technology
Graduate School of Medicine
Tohoku University, Japan

S. Sato, MD, PhD
Dept. of Neurology
Kohnan Hospital, Japan

H. Takata, MD, PhD · K. Nobukuni, MD, PhD
Dept. of Neurology
Minami Okayama National Hospital, Japan

S. Kuroda, MD, PhD*
Dept. of Neuropsychiatry
Graduate School of Medicine, Dentistry and Pharmaceutical Sciences
Okayama University, Japan

H. Takano, MD, PhD · Y. Umeda, MD, PhD
Dept. of Neurology
Brain Research Institute
Niigata University, Japan

H. Konno, MD, PhD
Dept. of Neurology
Nishitaga National Hospital, Japan

K. Nagasato, MD, PhD
Dept. of Neurology
Isahaya General Hospital, Japan

A. Satoh, MD, PhD
Dept. of Neurology
Nagasaki Kita Hospital, Japan

Y. Matsuda, MD, PhD
Dept. of Neuropsychiatry
Graduate School of Medicine
Yamaguchi University, Japan

M. Hidaka, MD, PhD
Yokohama Miyazaki Hospital of Neurosurgery, Japan

H. Takahashi, MD, PhD
Dept. of Neurology
Matsudo Municipal Hospital, Japan

Y. Sano, MD, PhD
Dept. of Neurology
Graduate School of Medicine
Yamaguchi University, Japan

K. Kim, MD, PhD
Dept. of Neurology
Shizuoka General Hospital, Japan

T. Konishi, MD, PhD
Dept. of Neurology
Shizuoka National Medical Center, Japan

K. Doh-ura, MD, PhD
Division of Prion Protein Biology
Graduate School of Medicine
Tohoku University, Japan

T. Sato, MD, PhD*
National Center for Neurology and Psychiatry
Kohnodai Hospital, Japan

K. Sasaki, MD, PhD
Dept. of Neuropathology
Neurological Institute
Graduate School of Medical Sciences
Kyushu University, Japan

Y. Nakamura, MD, PhD*
Dept. of Public Health
Jichi Medical School, Japan

M. Yamada, MD, PhD*
Depts. of Neurology and Neurobiology of Aging
Graduate School of Medical Science
Kanazawa University, Japan

H. Mizusawa, MD, PhD*
Dept. of Neurology and Neurological Science
Graduate School
Tokyo Medical and Dental University, Japan

* The Creutzfeldt-Jakob Disease Surveillance Committee, Japan.

JON 2540

☐ **Abstract** *Objective* To describe the clinical features of Creutzfeldt-Jakob disease with a substitution of arginine for methionine (M232R substitution) at codon 232 (CJD232) of the prion protein gene (PRNP). *Patients and methods* We evaluated the clinical and laboratory features of 20 CJD232 patients: age of onset, initial symptoms, duration until becoming akinetic and mute, duration until occurrence of periodic sharp and wave complexes on EEG (PSWC), MRI findings, and the presence of CSF 14-3-3 protein. Immunohistochemically, prion protein (PrP) deposition was studied. *Results* None of the patients had a family history of CJD. We recognized two clinical phenotypes: a rapidly progressive type (rapid-type) and a slowly progressive type (slow-type). Out of 20 patients, 15 became akinetic and mute, demonstrated myoclonus, and showed PSWC within a mean duration of 3.1, 2.4, and 2.8 months, respectively (rapid-type). Five showed slowly progressive clinical courses (slow-type). Five became akinetic and mute and four demonstrated myoclonus within a mean duration of 20.6 and 15.3 months, respectively, which were significantly longer than those in the rapid-type. Only one demonstrated PSWC 13 months after the onset. Diffuse synaptic-type deposition was demonstrated in four rapid-type patients, and perivacuolar and diffuse synaptic-type deposition in two, and diffuse synaptic-type deposition in one slow-type patient. Three of 50 suspected but non-CJD patients had the M232R substitution. *Conclusions* Patients with CJD232 had no family history like patients with sCJD, and showed two different clinical phenotypes in spite of having the same PRNP genotype. More studies are needed to determine whether M232R substitution causes the disease and influences the disease progression.

☐ **Key words** Creutzfeldt-Jakob disease · M232R · clinical phenotype · uncommon variant · diffusion-weighted MRI

Introduction

Human prion diseases are divided into three types: sporadic, genetic, and infectious prion disease. Genetic prion disease, which is defined as prion disease with causative abnormalities of the prion protein gene (PRNP), accounts for approximately 10 to 15% of all prion disease cases, and includes genetic Creutzfeldt-Jakob disease (gCJD), Gerstmann-Sträussler-Scheinker disease (GSS), and fatal familial insomnia (FFI) [1]. In general, the clinical features of gCJD are more various compared with those of sporadic CJD (sCJD) and are regulated by the genotype [2]. Therefore, gCJD, even if its clinical features are quite different from those of sCJD, especially those of the most often encountered type of sCJD with methionine homozygosity at codon 129 of PRNP and type 1 protease-resistant prion protein (MM1) [3], can be diagnosed by examining the genotype. To clarify the clinical features of CJD, which associates with a substitution in PRNP, will provide an important clue that can lead to genetic examination.

To date, more than 30 causative mutations have been recognized and individual PRNP mutations show variable geographical distribution and frequency. The cardinal characteristic of gCJD is that more than half of the patients lack family history.

CJD patients associated with a substitution of arginine for methionine at codon 232 (M232R substitution) in PRNP with no relevant family history have been reported in Japan [4–10]. Previously, the clinical features of CJD with the M232R substitution (CJD232) were thought to be similar to those of typical sCJD with MM1 [3], which accounts for the vast majority of sCJD in terms of clinical features, including EEG findings [5, 6, 9]. However, cases of CJD232 that showed a longer clinical course and lacked the characteristic periodic sharp and wave complexes (PSWC) have been reported [7, 8]. We have experienced eight cases of CJD232. Five of them showed a rapid clinical course and typical CJD features, while the others showed very slow progression and atypical features. We studied the clinical features of 20 CJD232 patients, including our original patients, and found that there were two different major clinical phenotypes with the same genotype, including polymorphisms at codons 129 and 219 of PRNP; one progressed rapidly, and the other progressed slowly. Better understanding of the clinical features of CJD232 would contribute to the diagnosis of CJD232, especially in patients with atypical clinical features.

Patients and methods

Twenty-four patients with CJD232 were included in this study: eight were our original cases, seven were obtained by reviewing the literature [5–10] and nine were found by reviewing the clinical records of CJD patients reported to the Creutzfeldt-Jakob disease Surveillance Committee, Japan. We excluded two patients because they had double point mutations at codon 180 and at codon 232 [10] and one patient because her polymorphism at codons 129 and 219 of PRNP was uncertain [5]. Therefore, 21 patients were enrolled in this study. The nine who were proven at autopsy are indicated by asterisks in Fig. 1.

We first evaluated the duration from onset until the patients manifested akinetic mutism. As shown in Fig. 1, 15 became akinetic and mute within six months, while five did not become so until 15 months after the onset. These CJD232 patients appeared to be comprised of two different groups: one was a rapidly progressive type (rapid-type) and the other was a slowly progressive type (slow-type). We evaluated the age of onset, initial symptoms, duration from onset to the appearance of myoclonus, duration from onset to akinetic mutism, du-

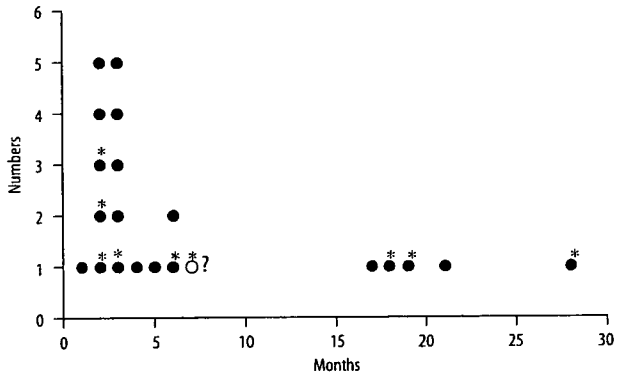

Fig. 1 The duration from the onset to akinetic mutism. The X-axis shows the duration (months) and the Y-axis shows the accumulative number of patients. Black circles indicate patients who became akinetic and mute; the white circle indicates a patient who had not become akinetic and mute. The white circle with a question mark indicates a 50-year-old-male patient who suddenly died seven months after the onset because of a myocardial incident. Since he had not become akinetic and mute, and was able to converse with simple words, we excluded him from further analyses. Asterisks indicate autopsy proven patients. We recognize two different groups concerning the duration from the onset to akinetic mutism: a rapidly progressive type and a slowly progressive type

ration from onset to occurrence of PSWC, results of MRI, and the presence of 14-3-3 protein in the CSF of the two types. The patient marked by a question mark in Fig. 1 was excluded from the evaluation. We were unable to determine which group this 50-year-old man belonged to because he had not become akinetic and mute and was still able to converse with simple words seven months after the onset when he suddenly died due to a myocardial incident [8]. Thus, the clinical data of 20 patients were finally used for this study.

In one of the rapid-type patients and in three of the slow-type patients including a previously reported 64-year-old woman [7], immunohistochemical staining of PrP using monoclonal antibody 3F4 (Prionics, Schlieren, Switzerland) was performed. Including the previously reported pathological findings of three patients belonging to the rapid-type [6], immunohistochemical staining of PrP in both groups were studied. In each group, the molecular type of the abnormal isoform of prion protein (PrP^{Sc}) was studied.

The Mann-Whitney U test was used for statistical comparison of the age of onset and the duration until the appearance of myoclonus and akinetic mutism from the onset between the rapid-type and the slow-type. The Grubbs-Smirnov critical test was used for statistical analysis of the duration until the appearance of PSWC from the onset between the rapid-type and the slow-type. Fisher's exact probability test was used for comparison of the male to female ratio, and the rates of myoclonus, akinetic mutism, and PSWC between the two types. It was also used for comparison of the positive rate of 14-3-3 immunoassay and MRI between the two types.

Results

Reviewing the clinical records of the enrolled patients, we found that no patients of either group had a family history of prion disease or dementia.

Fifteen patients, eight men and seven women, with a mean onset age of 65.4 ± 5.2 (Mean ± SD) years could be categorized as the rapid-type. Of those, seven with an initial symptom of progressive dementia or memory disturbance, two with visual symptoms, two with cerebellar ataxia, two with involuntary movement, and two with other symptoms. All except for one uncertain patient demonstrated myoclonus 2.4 ± 1.8 months after the onset. All became akinetic and mute within a mean duration of 3.1 ± 1.5 months, and demonstrated PSWC (Fig. 2A and B) within a mean duration of 2.8 ± 1.8 months. CJD-related high intensity lesions [11] were detected in eight of the nine patients examined by MRI. Similar to sCJD, three patterns existed: in one, high intensity lesions appeared mainly in the striatum (Fig. 3A); in another, they appeared in the striatum and the cortical ribbon equally (Fig. 3B); and in yet another, they appeared mainly in the cortical ribbon (Fig. 3C). The 14-3-3 protein assay was positive in all eight patients examined. All 15 patients showed MM129, 14 showed glutamic acid homozygosity at codon 219 (GG219) and one showed glutaminic acid/lysine heterozygosity at codon 219 in the PRNP analysis. These clinical features closely resembled typical sCJD with MM1 [3]. Immunohistochemical staining of PrP in four patients (one original patient and three previously reported patients [6]) revealed a diffuse synaptic-type deposit (Fig. 4A). The molecular type of PrP^{Sc} in one patient was type 1.

Five patients, two men and three women, with a mean onset age of 59.0 ± 12.8 years could be categorized as the slow-type. Three had an initial symptom of progressive dementia or memory disturbance, one showed psychiatric symptoms, and one had dressing apraxia. Four of five patients demonstrated myoclonus 15.3 ± 12.3 months after the onset, and the remaining one did not demonstrate myoclonus during the 13-month observation period. All became akinetic and mute within a mean duration of 20.6 ± 4.4 months. Only one demonstrated PSWC within the observation period of 23.8 ± 13.7 months (Fig. 2C and 2D). CJD-related high-intensity lesions were detected in four of the five patients examined by MRI [11]. One showed high-intensity lesions in the cortical ribbon (Fig. 3D and 3E), while in the others such lesions appeared in both the striatum and cortical ribbon (Fig. 3F). The medial thalami showed high-intensity lesions in all three patients examined by DWI (white arrows in Fig. 3D and E, and black arrows in Fig. 3F). The 14-3-3 protein assay was positive in all four patients examined. In the PRNP analysis, all five patients showed MM129 and GG219. Immunohistochemical staining in two patients revealed predominantly perivacuolar-type PrP deposits in the cerebral cortex (Fig. 4B), but also partly the diffuse synaptic-type deposits. In one patient, only the diffuse synaptic-type deposits were revealed. The molecular type of PrP^{Sc} in one patient who had predominantly perivacuolar-type PrP deposits was type 1 + 2.

Between the two groups, there were no differences in the age at onset, male to female ratio, or positive rate of

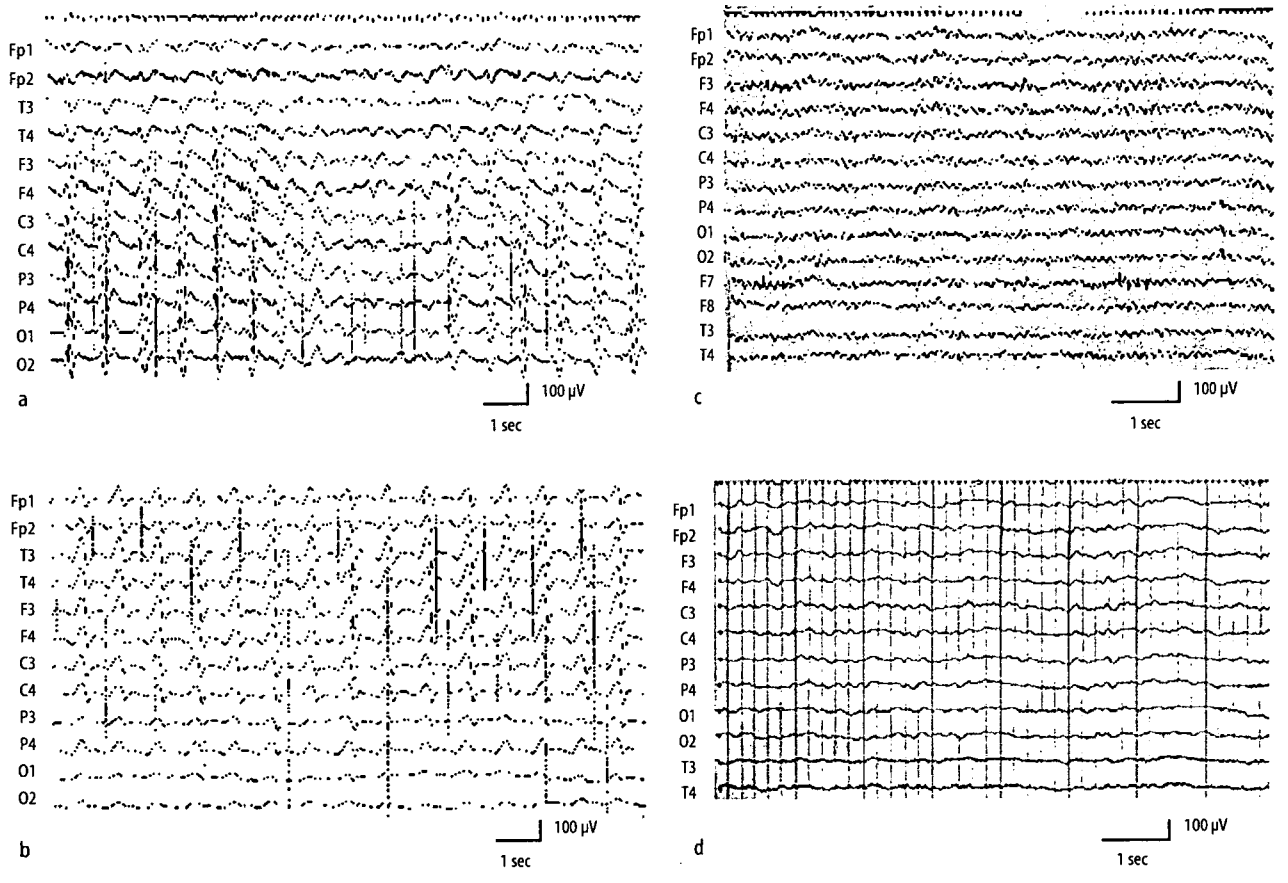

Fig. 2 EEG of representative patients of the rapid-type group and the slow-type group. **A** and **B** were recorded from the same 55-year-old woman in the rapid-type group. **C** and **D** were recorded from the same 69-year-old woman in the slow-type group. **A** EEG obtained two and half months after onset demonstrated high amplitude periodic sharp and wave complexes (PSWC) at a frequency of 1.5 Hz characteristic of CJD. **B** EEG obtained five months after the onset demonstrated PSWC at a frequency of 1 Hz. The amplitude was lower than that of Fig. 1A, and the background activities were flattened. EEG rapidly deteriorated. **C** EEG obtained four months after the onset. The background activities were 8 Hz mixed with no apparent slow activities. PSWC was not demonstrated. **D** EEG obtained twelve months after the onset. The background activities were 5 Hz mixed with δ activities. However, PSWC was not yet demonstrated

14-3-3 protein immunoassay. Similar to sCJD, there were three patterns of high-intensity lesions shown by MRI in the rapid-type. We were unable to distinguish the rapid-type of CJD232 from sCJD based on the clinical features including MRI findings. Patients with the slow-type did not have fewer lesions than patients with the rapid-type at diagnosis. High-intensity lesions in the medial thalamus depicted by DWI were a common finding of the slow-type (Fig. 3A–F). There was no difference in the rate of myoclonus between the two groups, but the duration until the appearance from the onset was longer in the slow-type compared with the rapid-type ($p < 0.005$). All patients became akinetic and mute in both types, but the duration until becoming akinetic and mute from the onset in the slow-type was longer than that in the rapid-type ($p < 0.001$). Concerning PSWC, all patients in the rapid-type demonstrated PSWC 2.8 ± 1.8 months after the onset. However, in the observation period of 21.6 ± 12.8 months, only one patient with the slow-type demonstrated PSWC 13 months after onset, which was later compared with that of the rapid-type ($p < 0.01$). The rate of PSWC in the slow-type was lower than that in the rapid-type ($p < 0.01$). Since there were no differences in the polymorphisms of codons 129 and 219 between the two groups, such polymorphisms would not be determinants of the disease subtype. Based on the differences in the clinical and laboratory findings (Table 1), we considered that these two types represented completely different phenotypes of exactly the same genotype.

By reviewing the investigative reports collected by the Creutzfeldt-Jakob Disease Surveillance Committee, Japan, as of February 2006, PRNP information was available from 511 patients: 317 were acknowledged as sporadic CJD, 41 as infectious CJD, 103 as genetic prion disease that included 28 CJD with V180I (CJD180), 27 GSS with P102L, 23 CJD with E200K, and 13 CJD232, and 50 as non-CJD. Three of the 50 non-CJD patients who had

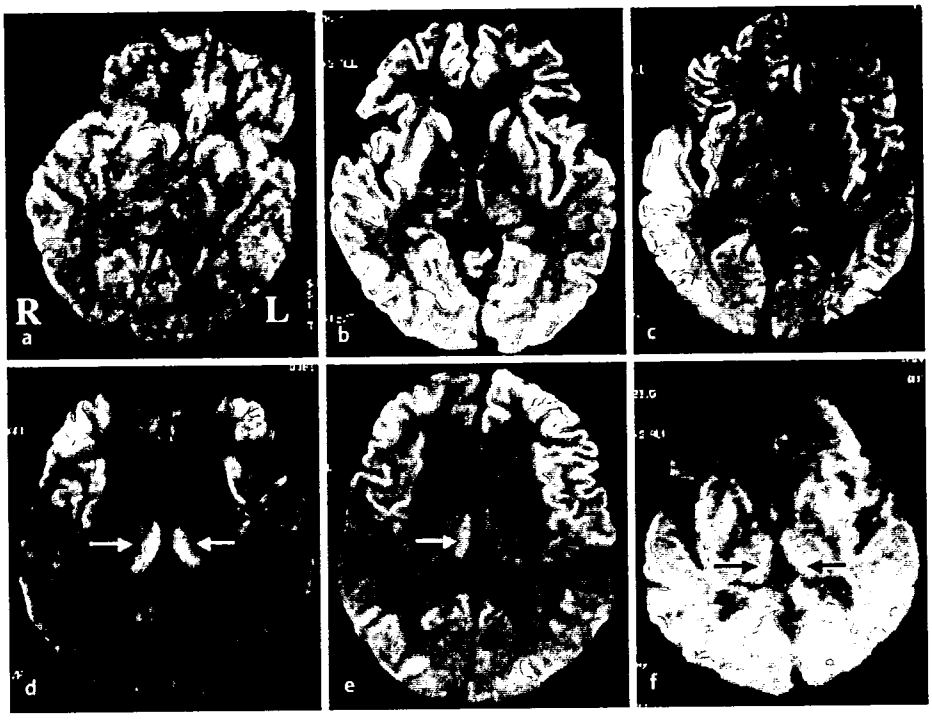

Fig. 3 DWI of the rapid-type group (**A–C**) and the slow-type group (**D–F**). **A** DWI obtained from a 55-year-old woman demonstrating high-intensity lesions mainly in the bilateral striatum. The right temporal cortex demonstrated slightly high-intensity lesions. **B** DWI obtained from a 60-year-old woman demonstrating high intensity lesions in the frontal, temporal, occipital and insular cortex, and the striatum. The right side predominated. **C** DWI obtained from a 62-year-old woman demonstrating high-intensity lesions in the bilateral occipital and insular cortex. The right temporal cortex was also depicted as an area of high intensity. We did not find high-intensity lesions in the striatum. **D** DWI obtained from a 69-year-old woman demonstrating high-intensity lesions in the bilateral frontal and insular cortex. The bilateral caudate head showed slightly high-intensity lesions. Interestingly, the bilateral medial thalami showed high-intensity lesions with the so-called hockey stick sign (white arrows). **E** DWI obtained from a 70-year-old man demonstrating high-intensity lesions in the bilateral frontal, occipital, and insular cortex. The right medial thalamus also showed high intensity (white arrow). **F** DWI obtained from a 52-year-old man demonstrating high-intensity lesions in the right temporal cortex and the left striatum. The bilateral medial thalami also showed high intensity lesion (black arrows)

no family history of prion disease had the M232R substitution: one was previously reported, pathologically confirmed dementia with Lewy bodies [12], one was encephalitis, and one was not diagnosed yet, but was confirmed as not having CJD because his symptoms rather fluctuated. There remains the possibility that the M232R substitution is a rare polymorphism, not a causative point mutation [6], although the M232R substitution was not found among 100 healthy controls [4].

Discussion

In the present study, by reviewing the clinical and laboratory findings of 21 patients, we found that there were two distinct phenotypes in CJD232 in spite of the same genotype of PRNP, M232R, MM129, and GG219. Different phenotypes with the same pathogenic changes of PRNP are known in several types of genetic prion disease [14–21]. Fatal familial insomnia and gCJD with a common point mutation at codon 178 are well-known. However, the different phenotypes are regulated by a polymorphism at codon 129 [14, 15]. Similarly, a phenotypic variant of gCJD with a point mutation of glutamic acid to lysine at codon 200 (CJD200) is coupled with valine at codon 129 [19]. On the other hand, a thalamic variant of CJD200, which has the same polymorphism of MM129 as the vast majority of CJD200, has been reported [17, 21], although it is exceptional. In our results, 15 of the patients were the rapid-type, five were the slow-type. In CJD232, the slow-type, which has uncommon clinical features, is not exceptional and constitutes one of the major phenotypes because 25% of patients with CJD232 belong to the slow-type. Similarly, there are two different major phenotypes that are not influenced by the polymorphism of codon 129 and 219 in Gerstmann-Sträussler-Scherinker disease with a point mutation of proline to leucine at codon 102 of PRNP (GSS102), which is characterized by chronic cerebellar ataxia of long duration (several years or more) associated with neurological signs including dementia [21]. In GSS102, a sCJD-like variant of short duration (less than one year) has been reported [16]. In 27 patients with GSS102 recognized by the Creutzfeldt-Jakob Disease Surveillance

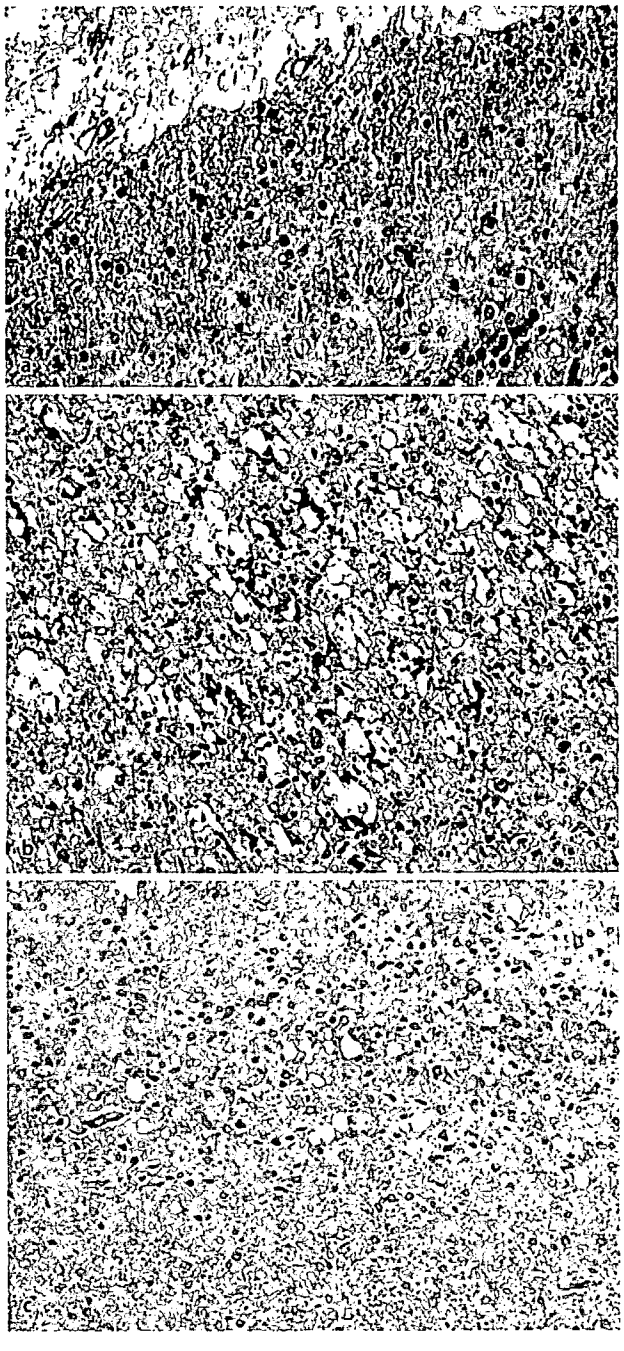

Fig. 4 Immunohistochemical staining of abnormal PrP using monoclonal antibody 3F4. **A** Anti-PrP immunostaining in a 67-year-old woman suffering from the rapid-type of CJD232 with an initial symptom of cerebellar ataxia. The molecular layer of the cerebellum shows a diffuse synaptic-type PrP deposit. Photographed at 200 times magnification. **B** Anti-PrP immunostaining in a 64-year-old woman suffering from the slow-type of CJD 232 with an initial symptom of dressing apraxia. This patient was previously reported by Satoh et al. (1997). The perivacuolar-type PrP deposit is predominantly demonstrated in the temporal cerebral cortex. Photographed at 50 times magnification. **C** Anti-PrP immunostaining in the same patient with Fig. 4B. The synaptic-type PrP deposit is demonstrated in the occipital cerebral cortex. Photographed at 50 times magnification

Committee, Japan until February 2006, five (18.5%) were this sCJD-like variant. It should be emphasized that CJD232 has two major different phenotypes with the completely same genotype of PRNP that is undoubtedly a major factor which influences the clinical phenotype [2, 22–24].

The gender and age at onset influence the disease progression [25]. However, there were no significant differences in the male to female ratio and age at onset between the two types in our series of CJD232. The molecular type of PrP^{Sc} is another factor that is closely associated with the clinical and pathological phenotypes of sCJD [26]. Unfortunately, the molecular type of PrP^{Sc} has not been sufficiently examined. One previously reported patient [27] in the rapid-type group had type 1 and one patient in the slow-type group had type 1 + 2. This difference may be a determinant of the clinical phenotypes of CJD232. More studies are needed to determine the relationship between the clinical phenotype and the molecular type of PrP^{Sc}. Immunohistochemical staining of PrP from four patients with the rapid-type revealed a diffuse synaptic-type deposit similar to that found in sCJD with MMI [28]. The synaptic-type PrP deposit may be an important pathological finding of the rapid-type. If so, we cannot differentiate the rapid-type of CJD232 from sCJD with MM1 based on the pathological findings. PrP immunohistochemical staining of three patients with the slow-type revealed that two had a perivacuolar-type and diffuse synaptic-type PrP deposits and one had only diffuse synaptic-type deposits. These pathological results suggest that the rapid-type might be a homogeneous group and the slow-type might not be. The number of studied patients in the two groups was too small to determine the pattern. If the PrP^{Sc} type 1 + 2 and the perivacuolar-type PrP deposits are key pathological features of the slow-type of CJD232, these may be related to the absence or late occurrence of myoclonus and PSWC on EEG, and the slower progression of the disease.

Diagnosing the rapid-type of CJD232 is not difficult because the patients start with progressing dementia, cerebellar ataxia, and visual problems, rapidly progress to akinetic mutism, demonstrate PSWC, are positive for 14-3-3 protein in the CSF immunoassay, and have characteristic MRI findings. These clinical features including the MRI findings are very similar to those of typical sCJD with MM1 [3] that accounts for the vast majority of sCJD. We can easily suspect CJD when we encounter such patients. Genetic examination of PRNP is necessary to differentiate the rapid-type of CJD232 from sCJD with MM1 [3] since a patient with CJD232 usually has no family history of prion disease or dementia, and differentiating CJD232 from sCJD with MM1 [3] is difficult when based on the clinical and laboratory features alone.

On the other hand, diagnosing the slow-type of

Table 1 Comparison of clinical and laboratory features between the rapid-type (R-type) and the slow-type (S-type) of CJD232

Clinical features	R-type (N = 15)	S-type (N = 5)	p
Age at onset (Year)	65.4 ± 5.2	59.0 ± 12.8	NS
Men: Women	8: 7	2: 3	NS
Family history	0/15 positive	0/5 positive	NS
Initial symptoms	7: progressive dementia 2: visual symptoms 2: cerebellar ataxia 2: involuntary movement 2: others	3: progressive dementia 1: psychiatric symptoms 1: dressing apraxia	
Myoclonus (Mo)[a]	2.4 ± 1.8	15.3 ± 12.3	< 0.005
Positive rate	14/14[b]	4/5*	NS
Akinetic mutism (Mo)[a]	3.1 ± 1.5	20.6 ± 4.4	< 0.001
Positive rate	15/15	5/5	NS
14-3-3 protein	8/8 positive	4/4 positive	NS
PSWC (Mo)[a]	2.8 ± 1.8	13	< 0.01
Positive rate	15/15	1/5**	< 0.01
MRI	8/9 positive	4/5 positive	NS
Codon 129	15: Met/Met	5: Met/Met	
Codon 219	14: Glu/Glu 1: Glu/Lys	5: Glu/Glu	
Autopsied cases	5/15	3/5	
PrP immunostaining	Synaptic: 4	Synaptic + Perivacuolar: 2 Synaptic: 1	
PrP type	Type 1: 1	Type 1 + 2: 1	

Values are means ± SD where applicable

[a] The duration until the appearance of myoclonus, akinetic mutism, and PSWC from the onset; [b] It was uncertain whether myoclonus had appeared or not in one patient

* Mean observation period was 14.8 ± 10.7 months; ** Mean observation period was 21.6 ± 12.8 months

R-type the rapid-type of CJD232; *S-type* the slow-type of CJD232; *PSWC* periodic sharp and wave complexes in EEG; *PRNP* prion protein gene; *Met/Met* methionine homozygosity; *Glu/Glu* glutamic acid homozygosity; *Glu/Lys* heterozygosity of glutamic acid and lysine; *NS* not significant

CJD232 is not easy because the patients initially manifest non-characteristic dementia or memory disturbance, or psychiatric symptoms as in other neurodegenerative disorders, progress relatively slowly, do not become akinetic and mute within a year, and do not demonstrate PSWC. When we diagnose the slow-type of CJD232, we cannot rely on PSWC, the presence of which is the most widely accepted diagnostic marker at the present time. In addition to the slow progression, the lack of a family history may cause this disease to be confused with other neurodegenerative disorders such as Alzheimer's disease, dementia with Lewy bodies, corticobasal degeneration, frontotemporal dementia, etc., especially in the early phase. MRI, especially DWI [11], is very useful to distinguish the slow-type of CJD232 from other neurodegenerative disorders, because the slow-type of CJD232 demonstrates CJD-related high-intensity lesions in DWI, whereas the above-mentioned neurodegenerative disorders do not demonstrate abnormal changes in signal intensities. There has been a report of suspected CJD patients who had M232R and in whom a final pathological diagnosis of dementia with Lewy bodies demonstrated no signal changes in DWI [12]. In our series of three patients with the slow-type examined by DWI, medial thalamic lesions were demonstrated. However, these lesions are not specific for the slow-type of CJD232, and we sometimes encounter them in sCJD [29]. The major differential diagnosis of the slow-type of CJD232 is sCJD with the MM2-cortical type [3], because the slow-type of CJD232 usually fulfills the previously advocated diagnostic criteria for sCJD with the MM2 cortical type [30]. It is hardly possible clinically to distinguish the slow-type of CJD232 from sCJD with the MM2 cortical type. However, the molecular type of PrP^{Sc} in one patient of the slow-type CJD232 was type 1 + 2, not type 2. The molecular types of PrP^{Sc} in each group may be different, although the presence of perivacuolar-type PrP deposits is also a finding of sCJD with the MM2-cortical type [3]. PRNP study is indispensable to distinguish between the two groups and molecular typing may be able to distinguish between them. We did not find any peculiar lesions of the slow-type such as a remarkable high intensity lesion in the cerebral cortex except for those in the medial occipital and cerebellar cortices which are characteristic of fCJD with a point mutation of valine to isoleucine at codon 180 (CJD180),

which is an unusual type of fCJD [13]. The degree of the abnormalities in MRI did not correlate with the disease severity. To diagnose the slow type of CJD232, recognizing the clinical phenotype that demonstrates uncommon clinical and laboratory features found in other neurodegenerative disorders with dementia and performing genetic examination of PRNP are important.

Other characteristics of CJD232 are that CJD232 patients have no family history of CJD or dementia in either type and are reported only in Japan. More than half of genetic prion disease patients with various PRNP mutations lack family histories and the lack of family histories is not restricted to CJD232 [1]. De novo mutations [31] and very low penetration [32] are considered as the reasons. Individual PRNP mutations also show variable geographical distributions [1]. The M232R substitution may influence the disease progression because the M232R substitution extended the incubation time in an experimental transmission study using humanized knock-in mice [33]. Three suspected patients with M232R substitution but with a final diagnosis of diseases other than CJD have been reported to the Creutzfeldt-Jakob Disease Surveillance Committee, Japan because they had the M232R substitution, not because they had clinical symptoms suspecting CJD. Therefore, we think that the prevalence of 6 % in 50 non-CJD patients is not the same as that of the normal Japanese population. At least, it cannot be said that all patients having the M232R substitution demonstrate the symptoms of CJD232, and it does not seem to be supported that M232R substitution is a causative mutation. On the other hand, two probable CJD patients with M232R substitution in one family have been reported [6]. We cannot overlook these patients based on the fact that M232R substitution is very rare [4]. Whether M232R is really a causative mutation or only a rare polymorphism is another issue that needs to be resolved. We need more studies of CJD patients with M232R substitution, and especially the correlation between the pathological findings including the molecular type of PrP^{Sc} and immunohistochemical staining of PrP and the clinical findings should be clarified to determine whether it influences the disease progression. We need to study the morbidity of a population having the M232R substitution to determine whether it is a causative mutation or not.

□ **Acknowledgement** We thank Mr. Brent Bell for reading the manuscript. We also wish to thank all the doctors for their care of the patients. This study was based on the fruits of the Creutzfeldt-Jakob Disease Surveillance Committee, Japan and was supported in part by a grant from the Research Committee on Prion Disease and Slow Virus Infection, Ministry of Labor and Health, Japan. Yusei Shiga, Tetsuyuki Kitamoto, Shigetoshi Kuroda, Takeshi Sato, Yoshikazu Nakamura, Masahito Yamada, and Hidehiro Mizusawa are the members of the Creutzfeldt-Jakob Disease Surveillance Committee, Japan. The surveillance study of the Creutzfeldt-Jakob Disease Surveillance Committee, Japan was approved by the ethics committee of Kanazawa University.

References

1. Kovács GG, Puopolo M, Ladogana A, et al. (2005) Genetic prion disease: the EUROCJD experience. Hum Genet 118:166–174
2. Kovács GG, Trabattoni G, Heinfellner JA, Ironside JW, Knight RSG, Budka H (2002) Mutations of the prion protein gene: Phenotypic spectrum. J Neurol 249:1567–1582
3. Parchi P, Giese A, Capellari S, et al. (1999) Classification of sporadic Creutzfeldt-Jakob disease based on molecular and phenotypic analysis of 300 subjects. Ann Neurol 46:224–233
4. Kitamoto T, Ohta M, Doh-ura K, Hitoshi S, Terao Y, Tateishi J (1993) Novel missense variants of prion protein in Creutzfeldt-Jakob disease or Gerstmann-Sträussler Syndrome. Biochem Biophys Res Commun 191:709–714
5. Shimizu T, Tanaka K, Tanahashi N, Fukuuchi Y, Kitamoto T (1994) Creutzfeldt-Jakob disease with a point mutation at codon 232 of prion protein – A case report. Clin Neurol 34: 590–592
6. Hoque MZ, Kitamoto T, Furukawa H, et al. (1996) Mutation in the prion protein gene at codon 232 in Japanese patients with Creutzfeldt-Jakob disease: a clinicopathological, immunohistochemical and transmission study. Acta Neuropathol 92:441–446
7. Satoh A, Goto H, Satoh H, et al. (1997) A case of Creutzfeldt-Jakob disease with a point mutation at codon 232: Correlation of MRI and neurological findings. Neurology 49:1469–1470
8. Saito T, Isozumi K, Komatsumoto S, Nara M, Suzuki K, Doh-ura K (2000) A case of codon 232 mutation-induced Creutzfeldt-Jakob disease visualized by the MRI-FLAIR images with atypical clinical symptoms. Clin Neurol 40: 51–54
9. Tagawa A, Natsuno T, Suzuki M, Ono S, Shimizu N (2001) Creutzfeldt-Jakob disease with codon 232 point mutation and showing myoclonus and PSD in the early stage. A case report. Neurol Med 54:161–165
10. Hitoshi S, Nagura H, Yamanouchi H, Kitamoto T (1993) Double mutations at codon 180 and codon 232 of the PRNP gene in an apparently sporadic case of Creutzfeldt-Jakob disease. J Neurol Sci 120:208–212
11. Shiga Y, Miyazawa K, Sato S, et al. (2004) Diffusion-weighted MRI abnormalities as an early diagnostic marker for Creutzfeldt-Jakob disease. Neurology 63:443–449
12. Koide T, Ohtake H, Nakajima T, et al. (2002) A patient with dementia with Lewy bodies and codon 232 mutation of PRNP. Neurology 59:1619–1621
13. Jin K, Shiga Y, Shibuya S, et al. (2004) Clinical features of Creutzfeldt-Jakob disease with V180I mutation. Neurology 62:502–505
14. Goldfarb LG, Peterson RB, Tabaton M, et al. (1992) Fatal familial insomnia and familial Creutzfeldt-Jakob disease: disease phenotype determined by a DNA polymorphism. Science 258: 806–808